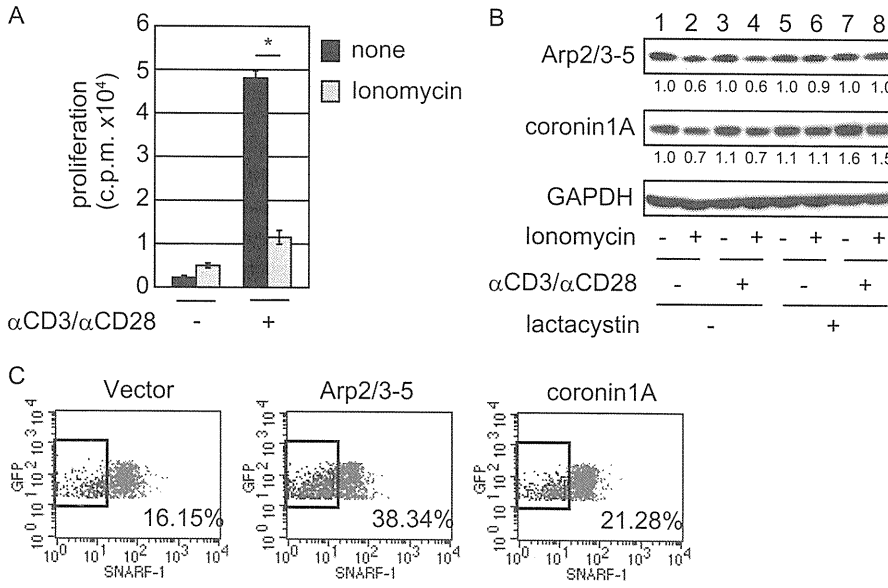

FIGURE 1. **Arp2/3-5 and coronin 1A are down-regulated in T cells anergized by ionomycin.** *A* and *B*, splenocytes derived from DO11.10 mice were stimulated with OVA for 3 days and rested for 7–10 days. The rested T cells were then treated with or without ionomycin for 18 h and restimulated with plate-bound anti-CD3 and soluble anti-CD28. *A*, proliferation was assessed by [^{3}H]thymidine uptake for 48 h. The mean c.p.m. of triplicate wells ± S.E. is shown (n = 9). *, p = 0.0000033 *versus* control. *B*, cells were lysed and analyzed by immunoblotting after 1-hour activation with plate-bound anti-CD3 and soluble anti-CD28. Each protein level analyzed by ImageJ software was normalized to the corresponding GAPDH level and is expressed as relative quantity to that of untreated control. *C*, DO11.10 CD4$^+$ T cells were transfected with vector control (GFP alone), Arp2/3-5, or coronin 1A. Forty-eight hours later, the transfected cells were treated with ionomycin for 18 h and were labeled with SNARF-1. The cells were restimulated with plate-bound anti-CD3 and soluble anti-CD28. Forty-eight hours later, proliferation was analyzed by FACS.

dence suggests that Cbl-b, which is E3 ligase as well as GRAIL, is important for induction of T cell anergy. We also analyzed whether Arp2/3-5 and coronin 1A are substrates of Cbl-b. However, Arp2/3-5 and coronin 1A are not ubiquitinated by Cbl-b (supplemental Fig. S1). These data indicate that GRAIL but not Cbl-b E3 ligase selectively ubiquitinates Arp2/3-5 and coronin 1A.

GRAIL Co-localizes with Arp2/3-5 and Coronin 1A—To address the interaction of Arp2/3-5 and coronin 1A with GRAIL, we examined the co-localization of these proteins. We transiently expressed GFP-tagged GRAIL together with HA-tagged ubiquitin and DsRed-tagged Arp2/3-5, coronin 1A, or RhoDGIα/β. After treatment with lactacystin, the localization of GRAIL and its substrates was analyzed by confocal microscopy. Indeed, Arp2/3-5 (Fig. 3*A*), coronin 1A (Fig. 3*B*), and RhoDGIα and β (Fig. 3, *C* and *D*) all co-localized with GRAIL. The substrates were localized together with GRAIL in contrast to the diffuse localization of GFP and substrate proteins in the cells transfected with GFP control vector and substrate proteins, indicating the co-localization of GRAIL and Arp2/3-5 or coronin 1A. These findings suggest that Arp2/3-5 and coronin 1A interact with GRAIL.

GRAIL Ubiquitinates Arp2/3-5 and Coronin 1A via Lys-63 and Lys-48—GRAIL has been reported to form polyubiquitin chains through lysine 63, resulting in proteolysis-independent functional modulation of Rho GDIs. However, when CD151 is the substrate, polyubiquitin chains are formed through lysine 48, which leads to protein degradation (18). We therefore assessed whether GRAIL ubiquitinates Arp2/3-5 and coronin 1A through Lys-63 and Lys-48. A similar polyubiquitinated ladder pattern of Arp2/3-5 was observed in the presence of WT Ub or Ub containing a lysine to arginine substitution at residue 29 (K29R) (Fig. 4*A*, *lanes 4* and *6*). In contrast, Ub conjugation of Arp2/3-5 was barely detected in the presence of Ub containing a lysine to arginine substitution at residue 48 (K48R) or at residue 63 (K63R) (Fig. 4*A*, *lanes 8* and *10*). Similarly, Ub conjugation of coronin 1A was observed in the presence of WT or K29R Ub (Fig. 4*B*, *lanes 4* and *6*) but was much lower when K48R or K63R Ub was used (Fig. 4*B*, *lanes 8* and *10*). These data reveal that Arp2/3-5 and coronin 1A were modified by Lys-48 and Lys-63 mixed linkage ubiquitin chains. To address the effect of GRAIL on the protein levels of Arp2/3-5 and coronin 1A, we overexpressed GRAIL and its enzymatically inactive mutant, H2N2-GRAIL or ΔRF-GRAIL, in DO11.10 CD4$^+$ T cells and determined Arp2/3-5 and coronin 1A expression by immunoblotting with specific Abs. Both Arp2/3-5 and coronin 1A were reduced when GRAIL, but not the enzymatically inactive forms of GRAIL, was overexpressed (Fig. 4*C*). These results indicate that GRAIL polyubiquitinates Arp2/3-5 and coronin 1A through Lys-48 and Lys-63 and eventually leads them to be degraded.

Less Arp2/3-5 and Coronin 1A Localize at the IS in Anergy—To investigate the role of Arp2/3-5 and coronin 1A in anergic T cells, we next examined the accumulation of F-actin, Arp2/3-5, and coronin 1A at the IS using confocal microscopy. As described previously, F-actin and Arp2/3-5 were recruited to the IS formed between DO11.10 CD4$^+$ T cells and $OVA_{323-339}$ peptide-pulsed A20 B cells (Fig. 5, *A* and *B*, *top panels*). In contrast, the accumulation of F-actin and the recruitment of Arp2/3-5 to the IS were reduced in ionomycin-treated DO11.10 CD4$^+$ T cells compared with those in control cells (Fig. 5*A*, *bottom panel*). Similarly, the recruitment of coronin 1A to the

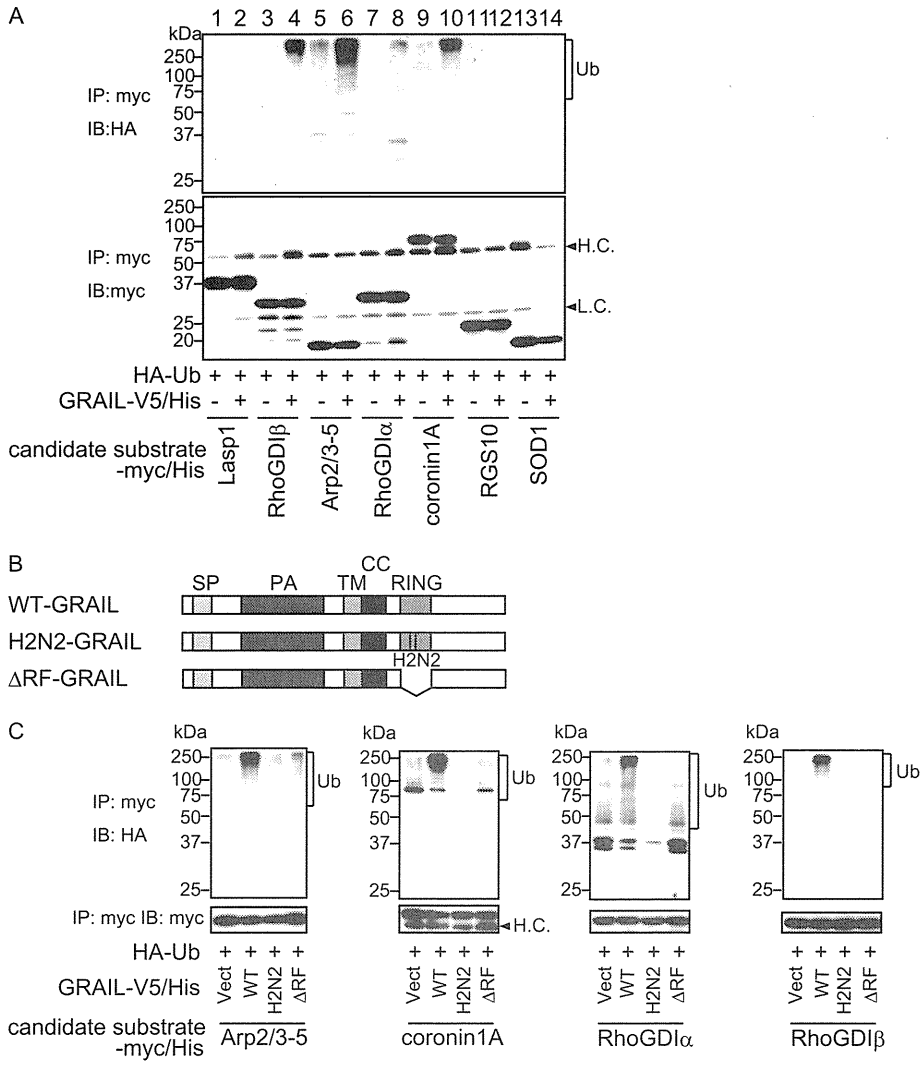

FIGURE 2. **Arp2/3-5 and coronin 1A are ubiquitinated by GRAIL.** *A* and *C*, HEK293T cells were transiently transfected with the indicated constructs and were treated with lactacystin for 12 h before lysis. Ubiquitination of the indicated proteins was detected by immunoprecipitation (*IP*) with anti-Myc Ab, followed by anti-HA immunoblotting (*IB*). The membrane was stripped and reprobed with anti-Myc Ab. *B*, schematic structures of the WT-, H2N2-, and ΔRF-GRAIL proteins.

IS in ionomycin-treated DO11.10 $CD4^+$ T cells was reduced compared with that in nontreated DO11.10 $CD4^+$ T cells (Fig. 5*B*, *bottom panel*). These data demonstrate that the accumulation of Arp2/3-5 and coronin 1A together with F-actin at the IS is impaired in anergic T cells.

GRAIL Inhibits Arp2/3 and Coronin 1A Accumulation at the IS—To address the contribution of GRAIL to IS formation, we overexpressed GRAIL, ΔRF-GRAIL, or a control vector in DO11.10 $CD4^+$ T cells and analyzed the accumulation of Arp2/3-5, coronin 1A, and F-actin at the IS. First, the expression of Arp2/3-5 and coronin 1A was reduced in T cells (GFP-positive cells) in which GRAIL was overexpressed compared with expression levels in control cells (Fig. 6, *A* and *B*, compare *top* and *middle panels*). The accumulation of both Arp2/3-5 and coronin 1A together with F-actin was reduced in DO11.10 $CD4^+$ T cells overexpressing GRAIL compared with that in control vector-transfected T cells (Fig. 6, *A* and *B*, compare *top* and *middle panels*). On the other hand, the accumulation of Arp2/3-5, coronin 1A, and F-actin at the IS in DO11.10 $CD4^+$ T cells overexpressing ΔRF-GRAIL was similar to that in controls (Fig. 6, *A* and *B*, *bottom panels*). We also examined whether the formation of IS occurred in ionomycin-treated T cells in which GRAIL was down-regulated by GRAIL shRNA-encoding retroviral infection. Coincident with the results for GRAIL-overexpressing experiments, both Arp2/3–5 and coronin 1A together with F-actin fully accumulated at the IS in ionomycin-treated GRAIL knockdown DO11.10 $CD4^+$ T cells compared with that in ionomycin-treated control T cells (anergic T cells) (supplemental Fig. S2). These results indicated that GRAIL regulates the recruitment of Arp2/3-5 and coronin 1A into the IS and the subsequent accumulation of F-actin at the site of the IS.

GRAIL Inhibits Lamellipodium Formation—Because Arp2/3 has been reported to be essential for the formation of lamellipodia at the IS, we next examined the effect of GRAIL on lamellipodium formation. Because the spreading of T cells on anti-TCR-coated coverslips requires the formation of stable actin structures and the generation of lamellipodia, we first analyzed whether T cells could spread onto anti-CD3-coated coverslips

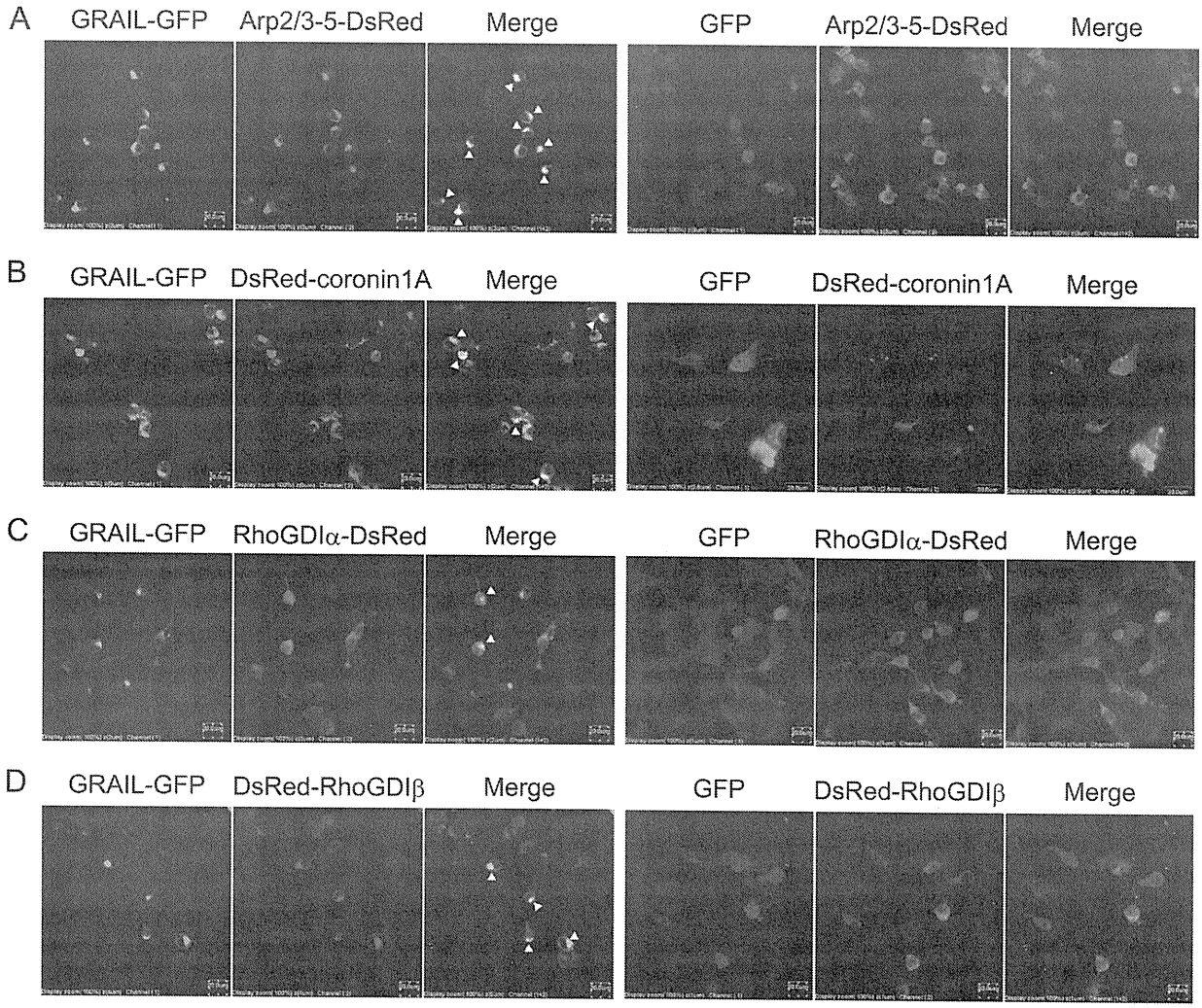

FIGURE 3. **GRAIL co-localizes with Arp2/3-5 and coronin 1A.** HEK293T cells were transiently transfected with constructs expressing GFP-tagged GRAIL, DsRed-tagged substrates (Arp2/3-5, *A*; coronin1A, *B*; RhoGDIα, *C*, and RhoGDIβ, *D*), and HA-ubiquitin and were treated with lactacystin for 12 h before being fixed. Co-localization with GFP-GRAIL was analyzed by confocal microscopy.

under anergic conditions. Control DO11.10 $CD4^+$ T cells spread onto anti-TCR-coated coverslips and formed round lamellipodial interfaces containing F-actin-rich structures (Fig. 7*A*). In contrast, DO11.10 $CD4^+$ T cells in which anergy had been induced by ionomycin barely formed lamellipodia (Fig. 7*A*, *bottom panels*). We next analyzed the lamellipodium formation in $CD4^+$ T cells overexpressing GRAIL. Lamellipodia were not efficiently formed on anti-CD3-coated coverslips when GRAIL was overexpressed in DO11.10 $CD4^+$ T cells (Fig. 7*B*, *middle panels*). In contrast, lamellipodia were efficiently formed at the IS when a catalytically inactive mutant GRAIL (ΔRF) was overexpressed in DO11.10 $CD4^+$ T cells (Fig. 7*B*, *bottom panels*). These data demonstrate that GRAIL inhibits lamellipodium formation at the IS.

DISCUSSION

In this study, we demonstrate that Arp2/3-5 and coronin 1A are down-regulated in anergic T cells as well as in T cells that overexpress GRAIL. Arp2/3-5 and coronin 1A co-localize with GRAIL and are ubiquitinated by GRAIL but not by Cbl-b via Lys-48 and Lys-63 linkage. Furthermore, the accumulation of Arp2/3-5 and coronin 1A together with F-actin is reduced at the IS in anergic T cells or in T cells that overexpress GRAIL. Coincident with the results for GRAIL-overexpressing experiments, IS formation in ionomycin-treated anergic T cells occurred by knockdown of GRAIL. Finally, we showed that overexpression of GRAIL suppresses lamellipodium formation at the IS.

CD40 ligand, CD151, CD83, and RhoGDI have been reported to be candidate substrates of GRAIL; however, the mechanism of GRAIL-mediated anergy induction is not yet fully understood (18–21). In fact, the expression of CD40 ligand was not up-regulated, and the down-regulation of CD3 was impaired in GRAIL-deficient mice. Because GRAIL is the only membrane protein among E3 ligases up-regulated in anergic T cells, it is reasonable that membrane proteins such as CD151 or CD83 are regulated by GRAIL. In this study, we confirmed that cytosolic proteins such as RhoGDIs serve as substrates for GRAIL. Fur-

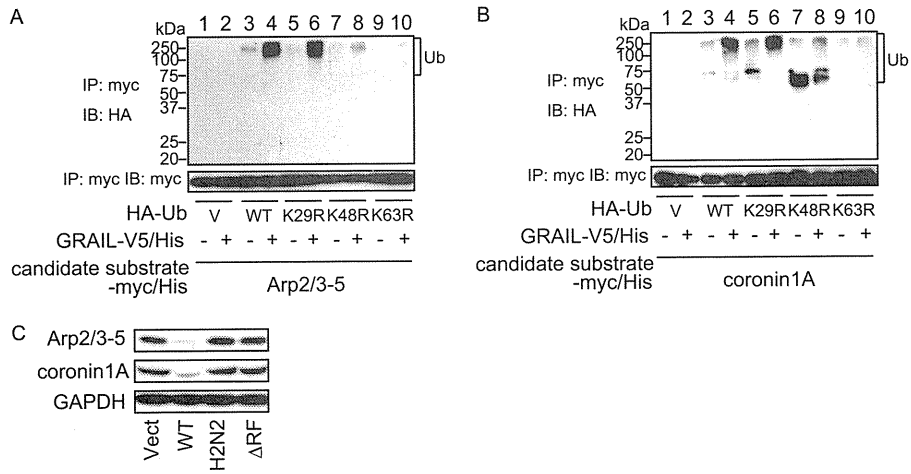

FIGURE 4. **Arp2/3-5 and coronin 1A are polyubiquitinated though Lys-48 and/or Lys-63 ubiquitin linkages and are down-regulated by catalytically active GRAIL.** *A* and *B*, HEK293T cells were transiently transfected with the indicated vectors and were treated with lactacystin for 12 h before lysis. Arp2/3-5 (*A*) and coronin 1A (*B*) were immunoprecipitated (*IP*) with anti-Myc Ab followed by immunoblotting (*IB*) with anti-HA Ab. The membrane was stripped and reprobed with anti-Myc Ab. *C*, $CD4^+$ T cells were transfected with vector control (GFP alone) or WT-, H2N2-, or ΔRF-GRAIL expression constructs. Forty-eight hours later, the transfected cells (GFP^+ cells) were sorted using a FACS Aria cell sorter. Sorted cells were rested for 2 days and were subjected to immunoblot analysis with anti-coronin 1A or Arp2/3-5 Ab.

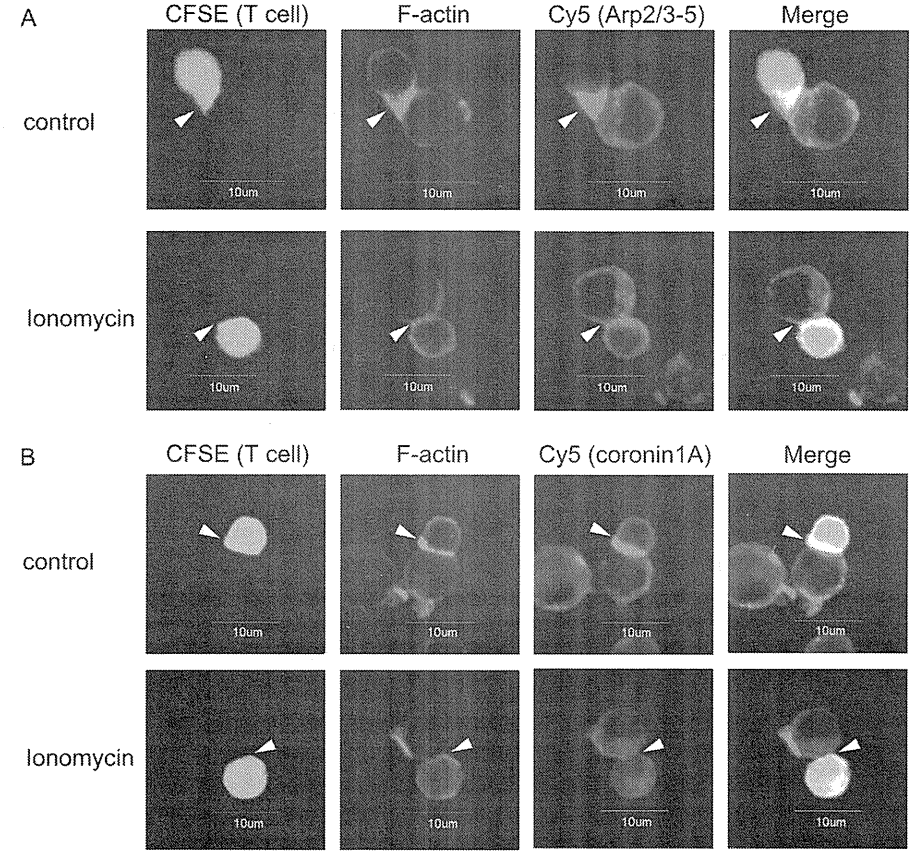

FIGURE 5. **The accumulation of Arp2/3-5, coronin 1A, and F-actin at the IS is reduced in anergic T cells.** *A* and *B*, OVA-stimulated DO11.10 splenocytes were rested for 7–10 days. Rested T cells were stained with CFSE, treated with or without ionomycin for 18 h, incubated with $OVA_{323-339}$-pulsed A20 cells, and co-stained with rhodamine-phalloidin (*red*) to visualize F-actin and either anti-Arp2/3-5 Ab (*A*) or anti-coronin 1A Ab (*purple*) (*B*). The *arrowheads* indicate IS.

thermore, we identified Arp2/3-5 and coronin 1A as novel substrates for GRAIL. Interestingly, these proteins as well as RhoGDIs are reportedly involved in the regulation of cytoskeletal organization. Although ubiquitination of target proteins was almost completely lost when either K63R or K48R mutant ubiquitin was used, it remains unclear whether Arp2/3-5 and coronin 1A are ubiquitinated via Lys-48, Lys-63, or both sites. To address this issue, characterization of ubiquitin chain using

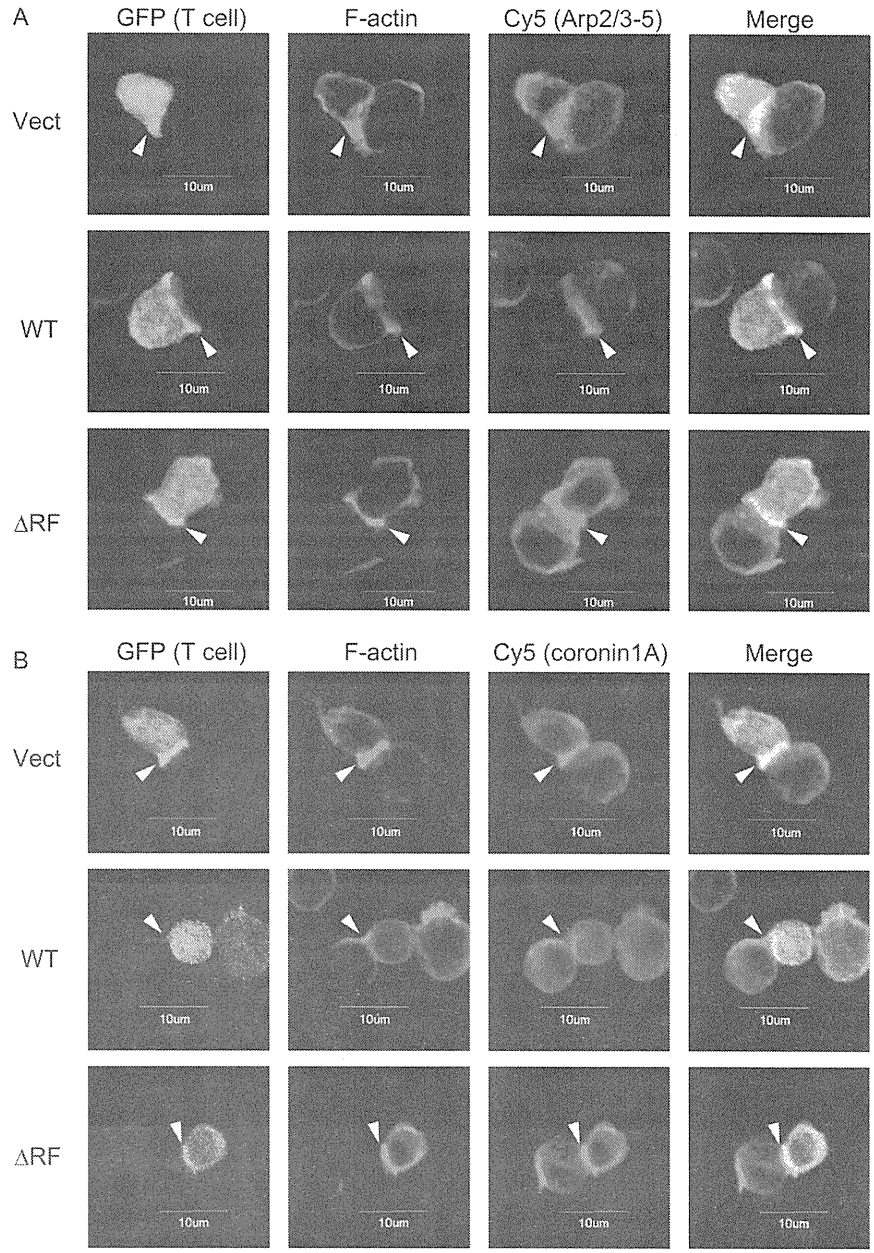

FIGURE 6. **GRAIL inhibits the accumulation of Arp2/3-5, coronin 1A, and F-actin at the IS.** *A* and *B*, DO11.10 $CD4^+$ T cells were transfected with vector control (GFP alone) or WT- or ΔRF-GRAIL expression constructs (*green*). Each population was incubated with $OVA_{323-339}$-pulsed A20 cells and co-stained with rhodamine-phalloidin (*red*) and either anti-Arp2/3-5 (*A*) or anti-coronin 1A (*purple*) (*B*). The *arrowheads* indicate IS.

MALDI-TOF-MS or mutants in which Lys-48 or Lys-63 is the only lysine residue that can mediate the ubiquitin chain formation will be needed for future studies

The immunological synapse is important in sustained signaling and delivery of a subset of effector cytokines by $CD4^+$ T cells (25, 29, 31, 32). Although the precise contribution of actin cytoskeletal remodeling to T cell signaling and biologic function is not completely understood, both anergic T cells and T cells overexpressing GRAIL have been reported to form unstable immunologic synapses (4, 38). Actin nucleation in T cells is induced by the WAVE2 complex (33) and the actin-nucleation-promoting factor WASPs, which are required to promote and stabilize interactions between T cells and APC *in vitro* and TCR clustering on artificial surfaces. WASPs bind to actin monomers, whereas the acidic stretch associates with the Arp2/3-5 complex (23, 34), a seven-subunit complex that has intrinsic actin-nucleating activity and is essential for polarization of F-actin at the IS (25, 35). In addition, co-localization of WASPs and the Arp2/3-5 complex at the interface between anti-CD3-coated beads and Jurkat T cells suggests that these cytoskeletal components are essential for the dynamics of the actin cytoskeleton and for T cell function (24). Arp2/3-5 is essential for the formation of a stable synapse by creating lamellipodia (25). Consistent with these findings, overexpression of GRAIL reduced the protein expression of Arp2/3-5 and impaired lamellipodium formation. These results suggest that proteins

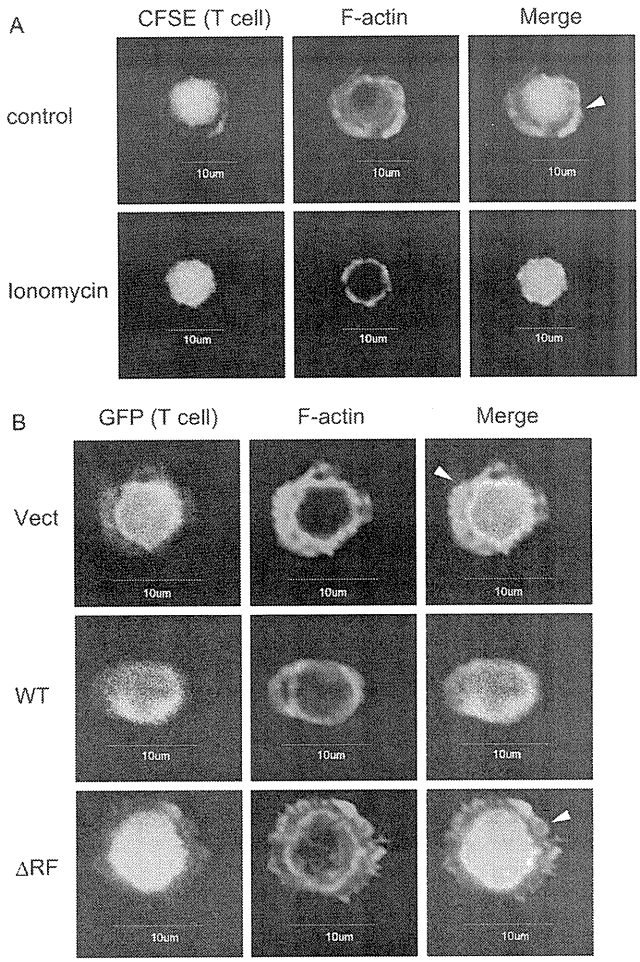

FIGURE 7. **GRAIL inhibits lamellipodium formation during TCR stimulation.** *A*, OVA-stimulated DO11.10 splenocytes were rested for 7–10 days and stained with CFSE. The cells were treated with or without ionomycin for 18 h. The cells were stimulated with plate-bound anti-CD3 mAb and stained with rhodamine-phalloidin (*red*) to visualize F-actin. *B*, DO11.10 $CD4^+$ T cells were transfected with a control vector (GFP alone) or WT- or ΔRF-GRAIL expression vectors. The cells were stimulated with coated anti-CD3 mAb and stained with rhodamine-phalloidin (*red*). The *arrowheads* indicate lamellipodium formation.

related to cytoskeletal reorganization at the IS are cytosolic targets for GRAIL.

An earlier study of coronin 1A knock-out mice reported that coronin 1A has an Arp2/3-5-dependent inhibitory effect on F-actin formation and concluded that coronin 1A is indispensable for TCR signaling (27, 29). In the present study, overexpression of coronin 1A restored the proliferative response. These findings suggest that coronin 1A participates in modulating T cell signaling and thereby contributes to the maintenance of anergy. In anergic T cells and in T cells overexpressing GRAIL, F-actin accumulation at the IS was decreased, although the expression of coronin 1A was reduced in contrast to previous studies. This may be because GRAIL regulates not only coronin 1A but also the Arp2/3-5 complex as well as RhoGDIs, which are important in the regulation of the accumulation of F-actin.

Anergic T cells have been reported to exhibit initial interaction, but implementation of T cell anergy results in reduced binding of LFA-1 to its ligand ICAM-1 (4). This process is mediated through degradation of PKC-θ and phospholipase C-γ by Cbl-b. A recent report demonstrated that overexpression of GRAIL impairs LFA-1 polarization at the IS (37). Stimulation through the TCR was shown to result in WAVE2-Arp2/3-5-dependent F-actin nucleation and the formation of a complex containing WAVE2, Arp2/3-5, vinculin, and talin (33). Moreover, TCR stimulation induces integrin clustering through the recruitment of vinculin and talin (33). Therefore, our study might link the unstable immunological synapse formation and impaired LFA-1 polarization at the IS in anergic T cells. Thus, whereas Cbl-b leads to unstable immunological synapse through degradation of tyrosine kinase, GRAIL leads to the phenotype of synapse disorganization via degradation of proteins involved in the actin cytoskeletal organization. In summary, we provide evidence that GRAIL regulates cytoskeletal reorganization to keep cells unresponsive to further antigen stimulation through the ubiquitination and down-regulation of the Arp2/3-5 complex and coronin 1A.

REFERENCES

1. Schwartz, R. H. (2003) *Annu. Rev. Immunol.* **21,** 305–334
2. Walker, L. S., and Abbas, A. K. (2002) *Nat. Rev. Immunol.* **2,** 11–19
3. Quill, H., and Schwartz, R. H. (1987) *J. Immunol.* **138,** 3704–3712
4. Heissmeyer, V., Macián, F., Im, S. H., Varma, R., Feske, S., Venuprasad, K., Gu, H., Liu, Y. C., Dustin, M. L., and Rao, A. (2004) *Nat. Immunol.* **5,** 255–265
5. Jeon, M. S., Atfield, A., Venuprasad, K., Krawczyk, C., Sarao, R., Elly, C., Yang, C., Arya, S., Bachmaier, K., Su, L., Bouchard, D., Jones, R., Gronski, M., Ohashi, P., Wada, T., Bloom, D., Fathman, C. G., Liu, Y. C., and Penninger, J. M. (2004) *Immunity* **21,** 167–177
6. Venuprasad, K., Elly, C., Gao, M., Salek-Ardakani, S., Harada, Y., Luo, J. L., Yang, C., Croft, M., Inoue, K., Karin, M., and Liu, Y. C. (2006) *J. Clin. Invest.* **116,** 1117–1126
7. Hsiao, H. W., Liu, W. H., Wang, C. J., Lo, Y. H., Wu, Y. H., Jiang, S. T., and Lai, M. Z. (2009) *Immunity* **31,** 72–83
8. Anandasabapathy, N., Ford, G. S., Bloom, D., Holness, C., Paragas, V., Seroogy, C., Skrenta, H., Hollenhorst, M., Fathman, C. G., and Soares, L. (2003) *Immunity* **18,** 535–547
9. Andoniou, C. E., Lill, N. L., Thien, C. B., Lupher, M. L., Jr., Ota, S., Bowtell, D. D., Scaife, R. M., Langdon, W. Y., and Band, H. (2000) *Mol. Cell Biol.* **20,** 851–867
10. Rao, N., Miyake, S., Reddi, A. L., Douillard, P., Ghosh, A. K., Dodge, I. L., Zhou, P., Fernandes, N. D., and Band, H. (2002) *Proc. Natl. Acad. Sci. U.S.A.* **99,** 3794–3799
11. Lupher, M. L., Jr., Rao, N., Lill, N. L., Andoniou, C. E., Miyake, S., Clark, E. A., Druker, B., and Band, H. (1998) *J. Biol. Chem.* **273,** 35273–35281
12. Lupher, M. L., Jr., Songyang, Z., Shoelson, S., Cantley, L. C., and Band, H. (1997) *J. Biol. Chem.* **272,** 33140–33144
13. Duan, L., Reddi, A. L., Ghosh, A., Dimri, M., and Band, H. (2004) *Immunity* **21,** 7–17
14. Fang, D., and Liu, Y. C. (2001) *Nat. Immunol.* **2,** 870–875
15. Liu, Y. C. (2004) *Annu. Rev. Immunol.* **22,** 81–127
16. Kriegel, M. A., Rathinam, C., and Flavell, R. A. (2009) *Proc. Natl. Acad. Sci. U.S.A.* **106,** 16770–16775
17. Nurieva, R. I., Zheng, S., Jin, W., Chung, Y., Zhang, Y., Martinez, G. J., Reynolds, J. M., Wang, S. L., Lin, X., Sun, S. C., Lozano, G., and Dong, C. (2010) *Immunity* **32,** 670–680
18. Lineberry, N. B., Su, L. L., Lin, J. T., Coffey, G. P., Seroogy, C. M., and Fathman, C. G. (2008) *J. Immunol.* **181,** 1622–1626
19. Lineberry, N., Su, L., Soares, L., and Fathman, C. G. (2008) *J. Biol. Chem.* **283,** 28497–28505
20. Su, L. L., Iwai, H., Lin, J. T., and Fathman, C. G. (2009) *J. Immunol.* **183,** 438–444

21. Su, L., Lineberry, N., Huh, Y., Soares, L., and Fathman, C. G. (2006) *J. Immunol.* **177,** 7559–7566
22. Holsinger, L. J., Graef, I. A., Swat, W., Chi, T., Bautista, D. M., Davidson, L., Lewis, R. S., Alt, F. W., and Crabtree, G. R. (1998) *Curr. Biol.* **8,** 563–572
23. Machesky, L. M., and Insall, R. H. (1998) *Curr. Biol.* **8,** 1347–1356
24. Krause, M., Sechi, A. S., Konradt, M., Monner, D., Gertler, F. B., and Wehland, J. (2000) *J. Cell Biol.* **149,** 181–194
25. Gomez, T. S., Kumar, K., Medeiros, R. B., Shimizu, Y., Leibson, P. J., and Billadeau, D. D. (2007) *Immunity* **26,** 177–190
26. Nolz, J. C., Gomez, T. S., Zhu, P., Li, S., Medeiros, R. B., Shimizu, Y., Burkhardt, J. K., Freedman, B. D., and Billadeau, D. D. (2006) *Curr. Biol.* **16,** 24–34
27. Föger, N., Rangell, L., Danilenko, D. M., and Chan, A. C. (2006) *Science* **313,** 839–842
28. Rodal, A. A., Sokolova, O., Robins, D. B., Daugherty, K. M., Hippenmeyer, S., Riezman, H., Grigorieff, N., and Goode, B. L. (2005) *Nat. Struct. Mol. Biol.* **12,** 26–31
29. Mugnier, B., Nal, B., Verthuy, C., Boyer, C., Lam, D., Chasson, L., Nieoullon, V., Chazal, G., Guo, X. J., He, H. T., Rueff-Juy, D., Alcover, A., and Ferrier, P. (2008) *PLos One.* **3,** e3467
30. Haraldsson, M. K., Louis-Dit-Sully, C. A., Lawson, B. R., Sternik, G., Santiago-Raber, M. L., Gascoigne, N. R., Theofilopoulos, A. N., and Kono, D. H. (2008) *Immunity.* **28,** 40–51
31. Bachmaier, K., Krawczyk, C., Kozieradzki, I., Kong, Y. Y., Sasaki, T., Oliveira-dos-Santos, A., Mariathasan, S., Bouchard, D., Wakeham, A., Itie, A., Le, J., Ohashi, P. S., Sarosi, I., Nishina, H., Lipkowitz, S., and Penninger, J. M. (2000) *Nature.* **403,** 211–216
32. Fang, D., Wang, H. Y., Fang, N., Altman, Y., Elly, C., and Liu, Y. C. (2001) *J. Biol. Chem.* **276,** 4872–4878
33. Nolz, J. C., Medeiros, R. B., Mitchell, J. S., Zhu, P., Freedman, B. D., Shimizu, Y., and Billadeau, D. D. (2007) *Mol. Cell Biol.* **27,** 5986–6000
34. Miki, H., Miura, K., and Takenawa, T. (1996) *EMBO J.* **15,** 5326–5335
35. Goley, E. D., and Welch, M. D. (2006) *Nat. Rev. Mol. Cell Biol.* **7,** 713–726
36. Deleted in proof
37. Schartner, J. M., Simonson, W. T., Wernimont, S. A., Nettenstrom, L. M., Huttenlocher, A., and Seroogy, C. M. (2009) *J. Biol. Chem.* **284,** 34674–34681
38. Mueller, P., Massner, J., Jayachandran, R., Combaluzier, B., Albrecht, I., Gatfield, J., Blum, C., Ceredig, R., Rodewald, H. R., Rolink, A. G., and Pieters, J. (2008) *Nat. Immunol.* **9,** 424–431

Cell Mol Neurobiol (2011) 31:1009–1020
DOI 10.1007/s10571-011-9698-x

ORIGINAL RESEARCH

Non-phosphorylated FTY720 Induces Apoptosis of Human Microglia by Activating SREBP2

Takashi Yoshino · Hiroko Tabunoki · Shigeo Sugiyama · Keitaro Ishii · Seung U. Kim · Jun-ichi Satoh

Received: 3 February 2011 / Accepted: 14 April 2011 / Published online: 26 April 2011

Abstract A synthetic analog of sphingosine named FTY720 (Fingolimod), phosphorylated by sphingosine kinase-2, interacts with sphingosine-1-phosphate (S1P) receptors expressed on various cells. FTY720 suppresses the disease activity of multiple sclerosis (MS) chiefly by inhibiting S1P-dependent egress of autoreactive T lymphocytes from secondary lymphoid organs, and possibly by exerting anti-inflammatory and neuroprotective effects directly on brain cells. However, at present, biological effects of FTY720 on human microglia are largely unknown. We studied FTY720-mediated apoptosis of a human microglia cell line HMO6. The exposure of HMO6 cells to non-phosphorylated FTY720 (FTY720-non-P) induced apoptosis in a dose-dependent manner with IC50 of 10.6 ± 2.0 μM, accompanied by the cleavage of caspase-7 and caspase-3 but not of caspase-9. The apoptosis was inhibited by Z-DQMD-FMK, a caspase-3 inhibitor, but not by Pertussis toxin, a Gi protein inhibitor, suramin, a S1P3/S1P5 inhibitor, or W123, a S1P1 competitive antagonist, although HMO6 expressed S1P1, S1P2, and S1P3. Furthermore, both phosphorylated FTY720 (FTY720-P) and SEW2871, S1P1 selective agonists, did not induce apoptosis of HMO6. Genome-wide gene expression profiling and molecular network analysis indicated activation of transcriptional regulation by sterol regulatory element-binding protein (SREBP) in FTY720-non-P-treated HMO6 cells. Western blot verified activation of SREBP2 in these cells, and apoptosis was enhanced by pretreatment with simvastatin, an activator of SREBP2, and by overexpression of the N-terminal fragment of SREBP2. These observations suggest that FTY720-non-P-induced apoptosis of HMO6 human microglia is independent of S1P receptor binding, and positively regulated by the SREBP2-dependent proapoptotic signaling pathway.

Keywords Apoptosis · Cholesterol · FTY720 · Microglia · S1P1 · SREBP2

Abbreviations

CNS	Central nervous system
DAVID	Database for Annotation, Visualization, and Integrated Discovery
EDG	Endothelial differentiation gene
FTY720-non-P	Non-phosphorylated form of FTY720
FTY720-P	Phosphorylated form of FTY720
G3PDH	Glyceraldehyde-3-phosphate dehydrogenase
GPCR	G-protein-coupled receptor
INSIG1	Insulin-induced gene 1
LDLR	Low density lipoprotein receptor

Electronic supplementary material The online version of this article (doi:10.1007/s10571-011-9698-x) contains supplementary material, which is available to authorized users.

T. Yoshino · H. Tabunoki · J. Satoh (✉)
Department of Bioinformatics and Molecular Neuropathology, Meiji Pharmaceutical University, 2-522-1 Noshio, Kiyose, Tokyo 204-8588, Japan
e-mail: satoj@my-pharm.ac.jp

S. Sugiyama · K. Ishii
Department of Chemistry of Functional Molecules, Meiji Pharmaceutical University, 2-522-1 Noshio, Kiyose, Tokyo 204-8588, Japan

S. U. Kim
Division of Neurology, Department of Medicine, University of British Columbia Hospital, University of British Columbia, Vancouver, BC, Canada

S. U. Kim
Medical Research Institute, Chung-Ang University College of Medicine, Seoul, Korea

MS	Multiple sclerosis
OPC	Oligodendroglial progenitor cell
S1P	Sphingosine-1-phosphate
SPHK2	Sphingosine kinase-2
SREBP	Sterol regulatory element-binding protein
PARP	Poly-ADP-ribose-polymerase
PTX	Pertussis toxin

Introduction

FTY720 (Fingolimod) is a synthetic analog of sphingosine generated by chemical modification of myriocin, a natural product of the fungus *Isaria sinclairii*. FTY720, phosphorylated by endogenous sphingosine kinase-2 (SPHK2), is converted into the biologically active form FTY720-P that binds to sphingosine-1-phosphate (S1P) receptors expressed on various cells (Brinkmann et al. 2010). S1P receptors belong to the endothelial differentiation gene (EDG) receptor family of G-protein-coupled receptors (GPCRs). FTY720-P interacts with S1P1, S1P3, S1P4, and S1P5 but not with S1P2. S1P1, S1P2, and S1P3 are distributed widely in the immune system, cardiovascular system, and the central nervous system (CNS), and S1P4 expression is more restricted to the lung, spleen, and thymus, while S1P5 is located chiefly on the skin, spleen, and brain. FTY720-P not only serves as an agonist for S1P receptors, but also acts as a functional antagonist for S1P1 by downregulating the receptor expression via internalization, ubiquitination, and proteasomal degradation (Mullershausen et al. 2009). The latter induces unresponsiveness to endogenous S1P.

Recent clinical trials indicate that FTY720 has promising therapeutic effects on multiple sclerosis (MS), a human demyelinating disease affecting exclusively the CNS white matter (Brinkmann et al. 2010). Oral administration of FTY720 reduces the number of gadolinium-enhanced lesions on MRI and decreased annual relapse rate in the patients with relapsing-remitting MS (Kappos et al. 2006). Consequently, US Food and Drug Administration (FDA) approved FTY720 as the first oral medication for MS in September 2010. FTY720-mediated immunomodulatory effects on the disease activity of MS are chiefly attributable to inhibition of S1P-dependent egress of autoreactive T lymphocytes from secondary lymphoid organs (Brinkmann et al. 2010).

Increasing evidence indicates that FTY720, capable of passing the blood–brain barrier due to its lipophilicity, exerts anti-inflammatory and neuroprotective effects within the CNS by interacting with a battery of S1P receptors expressed on neural cells (Dev et al. 2008). Reactive astrocytes in active MS lesions show a robust increase in S1P1 and S1P3 expression, where FTY720-P inhibits production of proinflammatory cytokines from astrocytes (Van Doorn et al. 2010). FTY720-P persistently downregulates S1P1 expression on astrocytes, and thereby attenuates the disease activity of experimental autoimmune encephalomyelitis (EAE), an animal model of MS (Choi et al. 2011). FTY720-P induces rapid phosphorylation of ERK1/2 and activates the PI3-kinase/Akt pathway in rat oligodendrocyte progenitor cells (OPCs), and subsequently protects OPCs from apoptosis caused by proinflammatory mediators (Coelho et al. 2007). FTY720-P promotes process extension of human OPCs and enhances their survival (Miron et al. 2008).

Microglia, acting as antigen-presenting cells and proinflammatory effector cells in the CNS, play a central role in development of demyelinating lesions in MS (Jack et al. 2005). Therefore, it is possible that FTY720 acts directly on microglia at the site of inflammation in MS brains. S1P1-expressing cells positive for CD68, a marker of microglia/macrophages, are accumulated in MS lesions (Van Doorn et al. 2010). Rat microglial cells express mainly S1P1 and S1P3 (Dev et al. 2008). In mouse organotypic cerebellar cultures affected with lysolecithin-induced demyelination, FTY720-P induces proliferation of microglia (Miron et al. 2010), while FTY720 reduces the accumulation of reactive microglia/macrophages in the lesions of traumatic brain injury (Zhang et al. 2007). FTY720 reduces the lesion size of cerebral infarct in mice with middle cerebral artery (MCA) occlusion and improves neurological deficits, accompanied by a decrease in the number of activated microglia/macrophages and apoptotic neurons (Wei et al. 2011). FTY720-P does not affect the global cytokine production by cultured human microglia (Durafourt et al. 2011). However, at present, immunomodulatory effects of FTY720 on human microglia remain largely unknown. The aim of the present study is to investigate biological effects of FTY720 on a human microglial cell line HMO6.

Methods

Human Microglia Cell Line HMO6

The HMO6 cell line was established by immortalizing cultured microglia isolated from human embryonic telencephalon tissues with a retroviral vector PASK1.2 encoding v-myc oncogene (Nagai et al. 2001). HMO6 cells express the markers of the microglia/macrophage lineage cells, including CD11b, CD68, CD86, HLA-ABC, HLA-DR, and ricinus communis agglutinin lectin-1 (RCA), serving as a model of human microglia both in

vitro and in vivo (Narantuya et al. 2010). The cells were maintained in Dulbecco's Modified Eagle's medium (DMEM; Invitrogen, Carlsbad, CA, USA) supplemented with 10% fetal bovine serum (FBS), 100 U/ml penicillin and 100 μg/ml streptomycin (feeding medium). Human neural and non-neural cell lines other than HMO6 were described elsewhere. LDH release from cultured cells was assessed by using a LDH cytotoxicity detection kit (Takara Bio, Shiga, Japan).

Chemicals

Non-phosphorylated FTY720 (FTY720-non-P; Calbiochem, Darmstadt, Germany) and *(S)*-FTY720 phosphate (FTY720-P; Echelon Biosciences, Salt Lake City, UT, USA) were usually dissolved in dimethyl sulfoxide (DMSO), providing the stock solution at the concentration of 10 mM. For negative controls, the inclusion of DMSO at the concentration of 0.1% v/v (1:1000 dilution) was applied. We found that the solvent alone never induces apoptosis of HMO6 at any incubation time. Sphingosine 1-phosphate (S1P) was obtained form Sigma, St. Louis, MO, USA. SEW2871, a selective S1P1 agonist and W123, a competitive S1P1 antagonist were obtained from Cayman Chemical, Ann Arbor, MI, USA. Suramin, a S1P3/S1P5 inhibitor, Z-DQMD-FMK, a caspase-3 inhibitor, and simvastatin, a HMG-CoA reductase inhibitor were obtained from Calbiochem. Pertussis toxin (PTX), a Gi protein inhibitor, was obtained form Seikagaku Biobusiness, Tokyo, Japan.

RT-PCR Analysis

Total cellular RNA was extracted by using TRIZOL (Invitrogen). RNA treated with DNase I was processed for cDNA synthesis using oligo$(dT)_{20}$ primers and SuperScript II reverse transcriptase (Invitrogen). Then, cDNA was amplified by PCR using HotStar Taq DNA polymerase (Qiagen, Valencia, CA, USA) and a panel of sense and antisense primer sets following: 5′aagcgctctttacttggtcgc tgg3′ and 5′tgatctccacccttcccagtgcat3′ for an 189 bp product of S1P1; 5′ccacagacctgggtgatgttg3′ and 5′tccccttaaatgctgcc tgcc3′ for a 200 bp product of S1P2; 5′actttgggctccagagtct ttc3′ and 5′cattctacgcacaggaaatgtagtg3′ for an 193 bp product of S1P3; 5′gttgcagtcttgcgtgtggatgg3′ and 5′ggtgac catgggaagcccatttg3′ for an 183 bp product of S1P4; 5′aggaatggcatgcgcaaag3′ and 5′cttctatggctcccacctcactc3′ for a 200 bp product of S1P5; and 5′ccatgttcgtcatgggtgtgaacca3′ and 5′gccagtagaggcagggatgatgttc3′ for a 251 bp product of the glyceraldehyde-3-phosphate dehydrogenase (G3PDH) gene.

For quantitative real-time RT-PCR (qPCR) analysis, cDNA was amplified by PCR in LightCycler ST300 (Roche Diagnostics, Tokyo, Japan) using SYBR Green I and a panel of sense and antisense primer sets with the following: 5′tgatcgttccagaagtggccttgg3′ and 5′aactgtcgtc ctatgttccccacc3′ for an 186 bp product of insulin-induced gene 1 (INSIG1) and 5′ctgggggtcttccttctatggaag3′ and 5′cacgtcatcctccagactgaccat3′ for an 168 bp product of low density lipoprotein receptor (LDLR). The expression levels of target genes were standardized against the levels of G3PDH, an internal control, detected in corresponding cDNA samples. All the assays were performed in triplicate.

Microarray Analysis

For microarray analysis, total cellular RNA was isolated by using the TRIZOL Plus RNA Purification kit (Invitrogen). The quality of total RNA was evaluated on Agilent 2100 Bioanalyzer (Agilent Technologies, Palo Alto, CA, USA). One hundred ng of total RNA was processed for cRNA synthesis, fragmentation, and terminal labeling with the GeneChip Whole Transcript Sense Target Labeling and Control Reagents (Affymetrix, Santa Clara, CA, USA). Then, it was processed for hybridization at 45°C for 17 h with Human Gene 1.0 ST Array that contains 28,869 genes (Affymetrix). The arrays were washed in the GeneChip Fluidic Station 450 (Affymetrix), and scanned by the GeneChip Scanner 3000 7G (Affymetrix). The raw data were expressed as CEL files and normalized by the robust multiarray average (RMA) method with the Expression Console software version 1.1 (Affymetrix). The annotation was studied by searching genes on the Database for Annotation, Visualization, and Integrated Discovery (DAVID) (david.abcc.ncifcrf.gov) (da Huang et al. 2009).

Molecular Network Analysis

KeyMolnet is a comprehensive knowledgebase that contains the contents on 123,000 relationships among human genes and proteins, small molecules, diseases, pathways and drugs, regularly updated, and curated by expert biologists (Satoh et al. 2009). By importing the list of Entrez Gene IDs derived from microarray data, KeyMolnet automatically provides corresponding molecules as a node on networks. Among various network-searching algorithms, the "neighboring" network-search algorithm selected one or more molecules as starting points to generate the network of all kinds of molecular interactions around starting molecules, including direct activation/inactivation, transcriptional activation/repression, and the complex formation within the designated number of paths from starting points. The generated network was compared side by side with 430 human canonical pathways of the KeyMolnet library. The algorithm counting the number of overlapping molecular relations between the extracted network and the

canonical pathway makes it possible to identify the canonical pathway showing the most significant contribution to the extracted network. The significance in the similarity between both is scored following the formula, where O = the number of overlapping molecular relations between the extracted network and the canonical pathway, V = the number of molecular relations located in the extracted network, C = the number of molecular relations located in the canonical pathway, T = the number of total molecular relations, and the X = the sigma variable that defines coincidence.

$$\text{Score} = -\log_2(\text{Score(p)}) \quad \text{Score (p)} = \sum_{x=O}^{Min(C,V)} f(x)$$

$$f(x) = {}_{C}C_{x} \cdot {}_{T-C}C_{V-x} / {}_{T}C_{V}$$

Transient Expression of SREBP2

To transiently overexpress sterol regulatory element-binding protein-2 (SREBP2), the gene encoding the N-terminal fragment of SREBP2 spanning amino acid residues 1–484 was amplified by PCR using PfuTurbo DNA polymerase (Stratagene, La Jolla, CA) and a sense and antisense primer set of 5′gcgatggacgacagcggcgagctg3′ and 5′tcacagaagaatccg tgagcggtc3′, and cloned in the expression vector pEF6 (Invitrogen). The vector was transfected into HMO6 cells by X-tremeGENE HP DNA transfection reagent (Roche Diagnostics). At 24 h after transfection, the cells were processed for western blot analysis. For the control, V5-tagged LacZ cloned in the pEF6 vector was transfected into sister cultures.

Western Blot Analysis

To prepare total protein extract, the cells were homogenized in RIPA buffer supplemented with a cocktail of protease inhibitors (Sigma). The protein extract was centrifuged at 12,000 rpm for 5 min at room temperature (RT). The protein concentration was determined by a Bradford assay kit (BioRad Hercules, CA, USA). The mixture of the supernatant and a 2× Lammeli loading buffer was boiled and separated on SDS-PAGE gels ranging from 8 to 12%. After gel electrophoresis, the protein was transferred onto nitrocellulose membranes, and immunolabeled at RT overnight with rabbit anti-poly-ADP-ribose-polymerase (PARP) antibody (#11835238001; Roche Diagnostics), rabbit anti-cleaved caspase-3 (Asp175) antibody (#9661; Cell Signaling Technology, Danvers, MA, USA), mouse anti-caspase-7 antibody (#9494; Cell Signaling Technology), rabbit anti-caspase-9 antibody (#9502; Cell Signaling Technology), rabbit anti-S1P1 antibody (sc-25489, EDG-1, H-60; Santa Cruz Biotechnology, Santa Cruz, CA), or goat anti-SREBP2 antibody (sc-8151, N-19; Santa Cruz Biotechnology). Then, the membranes were incubated at RT for 60 min with HRP-conjugated anti-mouse IgG, anti-rabbit IgG, or anti-goat IgG (Santa Cruz Biotechnology). The specific reaction was visualized by exposing the membranes to a chemiluminescent substrate (Thermo Scientific, Rockford, IL, USA).

In some experiments, the antibodies were stripped by incubating the membranes at 50°C for 30 min in stripping buffer, composed of 62.5 mM Tris-HCl, pH 6.7, 2% SDS, and 100 mM 2-mercaptoethanol. Then, the membranes were processed for relabeling with goat anti-heat shock protein HSP60 antibody (sc-1052, N-20; Santa Cruz Biotechnology) used for an internal control of protein loading, followed by incubation with HRP-conjugated anti-goat IgG.

Results

S1P Receptor Expression on Human Microglia Cell Line HMO6

The expression of five S1P receptor mRNAs in a panel of human neural cells and tissues was determined by RT-PCR. All the cells and tissues examined, including the human cerebrum (CBR), fetal astrocytes (AS), neuronal progenitor (NP) cells, NTera2 teratocarcinoma-derived neurons, SK-N-SH neuroblastoma, IMR-32 neuroblastoma, U-373MG astroglioma, and the microglia cell line HMO6, expressed varying levels of S1P1, S1P2, and S1P3 mRNAs, except for Y79 retinoblastoma that did not express S1P1 (Fig. 1a–c, lanes 2–10). In contrast, the levels of G3PDH, a housekeeping gene, were almost constant in the cells and tissues examined (Fig. 1f, lanes 2–10). Although discernible levels of S1P4 and S1P5 mRNAs were identified in the human cerebrum (CBR), both of these mRNAs were almost undetectable in HMO6 (Fig. 1d, e, lanes 2 and 10). No products were amplified when the reverse transcription step is omitted (Fig. 1a–f, lane 1). We verified S1P1 protein expression in HMO6 by western blot (not shown).

Non-Phosphorylated FTY720 Induced Apoptosis of HMO6

A 6 h-exposure of non-phosphorylated FTY720 (FTY720-non-P) induced LDH release from HMO6 cells and cell death in a dose-dependent manner with IC50 of 10.6 ± 2.0 μM (Fig. 2a, c). It is worthy to note that the concentration of FTY720-non-P at lower than 5 μM was completely ineffective in inducing cell death of HMO6 (Fig. 2a). Generally, LDH release did not discriminate apoptotic and necrotic cell death. The exposure of FTY720-non-P at a concentration of 10 μM mediated the cleavage of PARP in the incubation time longer than 4 h,

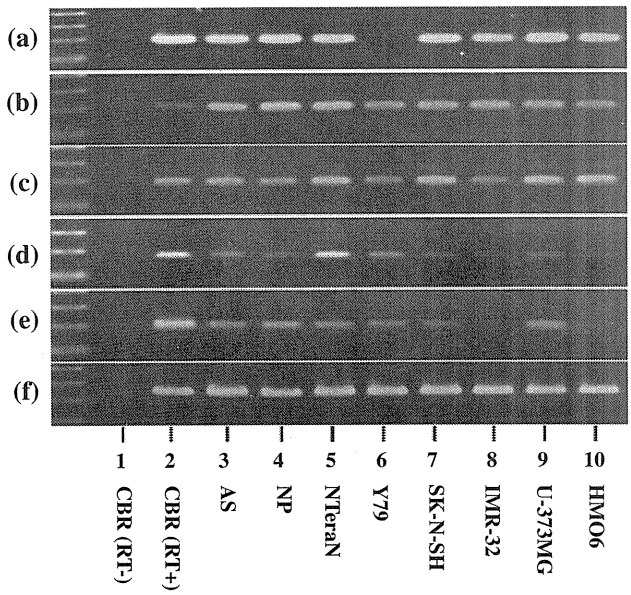

Fig. 1 S1P receptor expression in human neural cell lines. The expression of five S1P receptor mRNAs was studied by RT-PCR. **a** S1P1, **b** S1P2, **c** S1P3, **d** S1P4, **e** S1P5, and **f** G3PDH. The lanes (*1–10*) represent (*1*) the human frontal cerebral cortex (CBR) without inclusion of the reverse transcription (RT) step, (*2*) CBR with inclusion of the RT step, (*3*) cultured astrocytes (AS), (*4*) cultured neuronal progenitor (NP) cells, (*5*) NTera2 teratocarcinoma-derived neurons (NTera2N), (*6*) Y79 retinoblastoma, (*7*) SK-N-SH neuroblastoma, (*8*) IMR-32 neuroblastoma, (*9*) U-373MG astrocytoma, and (*10*) HMO6 microglia. The 100 bp ladder marker is shown on the left

indicating that FTY720-non-P induced cell death of HMO6 via apoptosis (Fig. 2d, lanes 7–10).

FTY720-non-P-induced apoptosis of HMO6 was accompanied by the cleavage of caspase-7 and caspase-3 (Fig. 3b, c, lane 2) but not of caspase-9 (Fig. 3e, lane 4), suggesting that the mitochondrial pathway of apoptosis that usually activates caspase-9 did not play a major role. Furthermore, Z-DQMD-FMK, a caspase-3-specific inhibitor, completely blocked FTY720-non-P-induced apoptosis of HMO6 (Fig. 3g, h, lane 10).

FTY720-Induced Apoptosis of HMO6 was Independent of S1P Receptor Binding

Because FTY720, when phosphorylated, binds to S1P1, S1P3, S1P4, and S1P5, all of which are G protein-coupled receptors (GPCR), we utilized Pertussis toxin (PTX), a Gi protein inhibitor, suramin, a S1P3/S1P5 inhibitor, and W123, a S1P1 competitive antagonist to block the ligand-receptor interaction. However, none of these receptor blockers could inhibit FTY720-induced apoptosis of HMO6 (Fig. 4a, lanes 4, 6, 8). Furthermore, SEW2871, a S1P1 selective agonist, and phosphorylated FTY720 (FTY720-P) at a concentration of 10 μM each did not induce apoptosis of HMO6 during the incubation time of 12 h (Fig. 4c, lanes 11 and 12). In addition, the combined administration of FTY720-P (10 μM) and FTY720-non-P (10 μM) did not inhibit apoptosis of HMO6, and treatment with sphiongosine-1 phosphate (S1P) (10–50 μM) did not induce apoptosis of HMO6 (data not shown). These results suggest that FTY720-non-P-induced apoptosis of HMO6 was independent of S1P receptor binding, and both FTY720-P and S1P were incapable of inducing apoptosis of HMO6.

FTY720 Induced SREBP-Responsive Genes

To investigate the molecular mechanism responsible for triggering FTY720-non-P-induced apoptosis of HMO6, we studied the genome-wide gene expression profile by microarray analysis. We identified 30 genes with an over 2-fold increase in HMO6 cells treated for 2 h with 10 μM FTY720-non-P versus those exposed to the vehicle (DMSO) (Table 1). Among them, the DAVID program categorized seven genes as a group of the genes associated with steroid and/or sterol metabolism (Table 1). None of apoptosis initiator and executor genes were induced in HMO6 cells at 2 h after initiation of the treatment. Upregulated expression of INSIG1 and LDLR in FTY720-non-P-treated HMO6 cells was validated by qPCR analysis (Fig. 5a, b).

Next, we imported the list of Entrez Gene IDs of the 30 genes upregulated in FTY720-non-P-treated HMO6 cells into KeyMolnet, a tool for analyzing molecular interactions on the comprehensive knowledgebase. KeyMolnet generated the molecular network, presenting with the most significant relationship with transcriptional regulation by sterol regulatory element-binding protein (SREBP) (the score = 69.719 with the *P*-value = 1.029E−21) (Fig. 5c). These results suggest that in HMO6 cells, FTY720-non-P activates SREBP proteins, either SREBP1 or SREBP2, belonging to the bHLH-Zip transcription factor family that promotes the synthesis of enzymes involved in cholesterol and fatty acid biosynthesis. To exclude a direct effect of vehicle (DMSO), in which FTY720-non-P was dissolved, on gene expression, we performed an additional set of microarray experiment by exposing HMO6 cells to FTY720-non-P dissolved in ethanol. We again identified the similar gene expression profile composed of upregulation of key SREBP-target genes, regardless of the solvent (See Table 1 in Electronic Supplementary Material).

SREBP2 is primarily involved in cholesterol synthesis, while SREBP1 chiefly regulates fatty acid synthesis (Sato 2010). INSIG1 identified by microarray analysis encodes an ER protein that plays a pivotal role in regulating intracellular cholesterol levels by interacting with SREBP cleavage-activating protein (SCAP) having the sterol-sensing domain activated by reduced cellular cholesterol levels. Thereafter, we have focused on SREBP2 expression

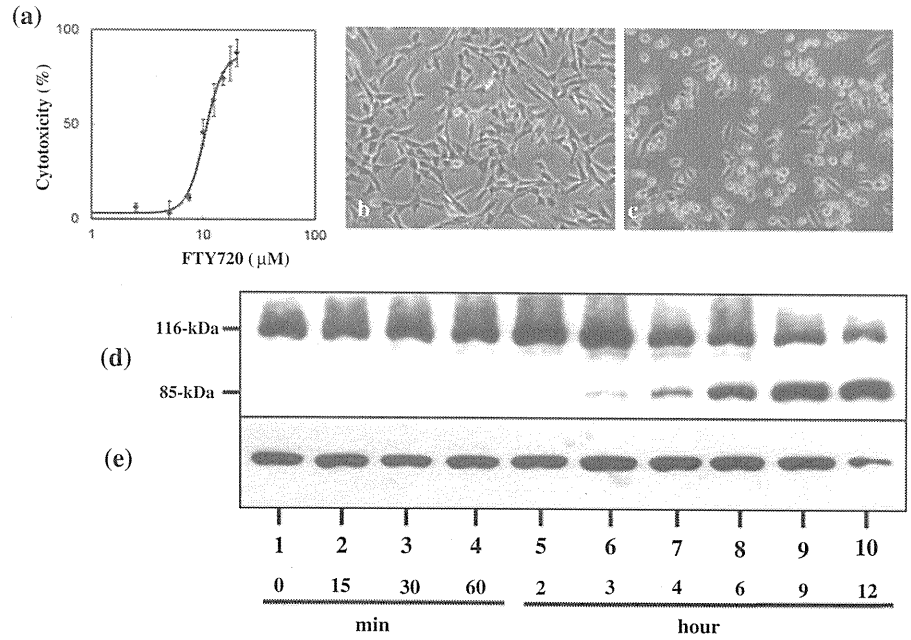

Fig. 2 Non-phosphorylated FTY720 induced apoptosis of HMO6 cells. HMO6 cells were exposed for various time periods to varying concentrations of non-phosphorylated FTY720 (FTY720-non-P). **a** LDH release assay, **b** the phase contrast photomicrograph of the cells exposed for 6 h to vehicle (DMSO), **c** the phase contrast photomicrograph of the cells exposed for 6 h to 10 μM FTY720-non-P, **d** western blot of PARP (an 116-kDa uncleaved form and an 85-kDa cleaved form), and **e** western blot of HSP60, an internal control of protein loading. The lanes (*1–10*) represent (*1*) untreated HMO6 cells, and HMO6 cells treated for (*2*) 15 min, (*3*) 30 min, (*4*) 1 h, (*5*) 2 h, (*6*) 3 h, (*7*) 4 h, (*8*) 6 h, (*9*) 9 h, and (*10*) 12 h with 10 μM FTY720-non-P

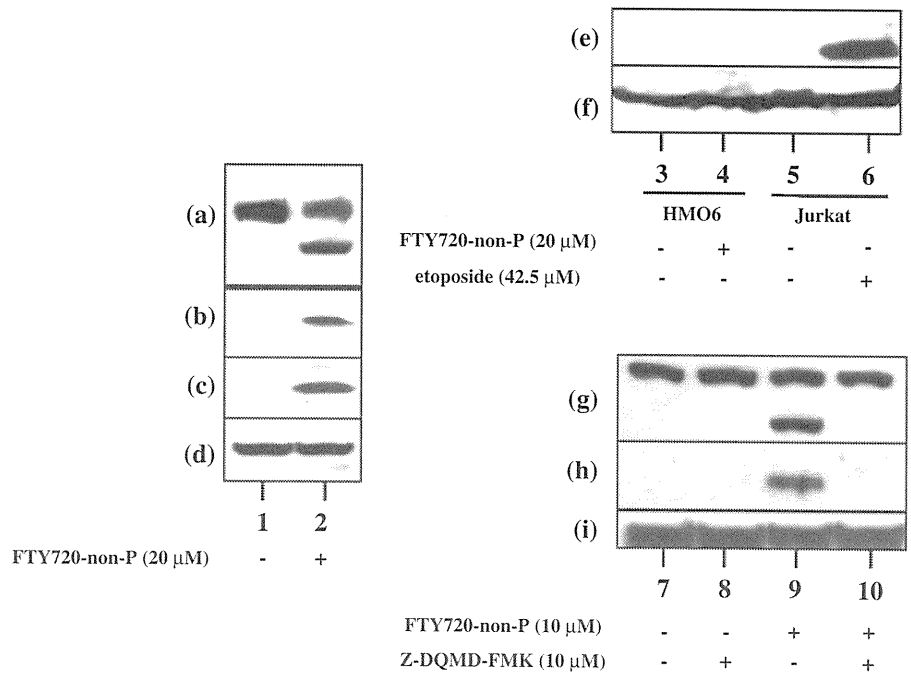

Fig. 3 FTY720-induced apoptosis of HMO6 was accompanied by activation of caspases 3 and 7. HMO6 cells were exposed for various time periods to varying concentrations of FTY720-non-P. For the positive control of caspase-9 activation, Jurkat cells were exposed to etoposide, an apoptosis-inducing agent. **a–i** indicate western blot of **a**, **g** PARP, **b** caspase-7 (a 20-kDa cleaved form), **c**, **h** caspase-3 (a 19-kDa cleaved form), **e** caspase-9 (a 37-kDa cleaved form), and **d**, **f**, **i** HSP60, an internal control of protein loading. The lanes (*1–10*) indicate HMO6 cells treated with (*1*, *3*) vehicle (DMSO) and (*2*, *4*) 20 μM FTY720-non-P for 9 h, and Jurkat cells treated with (*5*) vehicle (DMSO) and (*6*) 42.5 μM etoposide for 6 h, and (*7*) untreated HMO6 cells, and HMO6 cells treated with (*8*) 10 μM Z-DQMD-FMK, (*9*) 10 μM FTY720-non-P, and (*10*) a combination of 10 μM Z-DQMD-FMK and 10 μM FTY720-non-P for 12 h

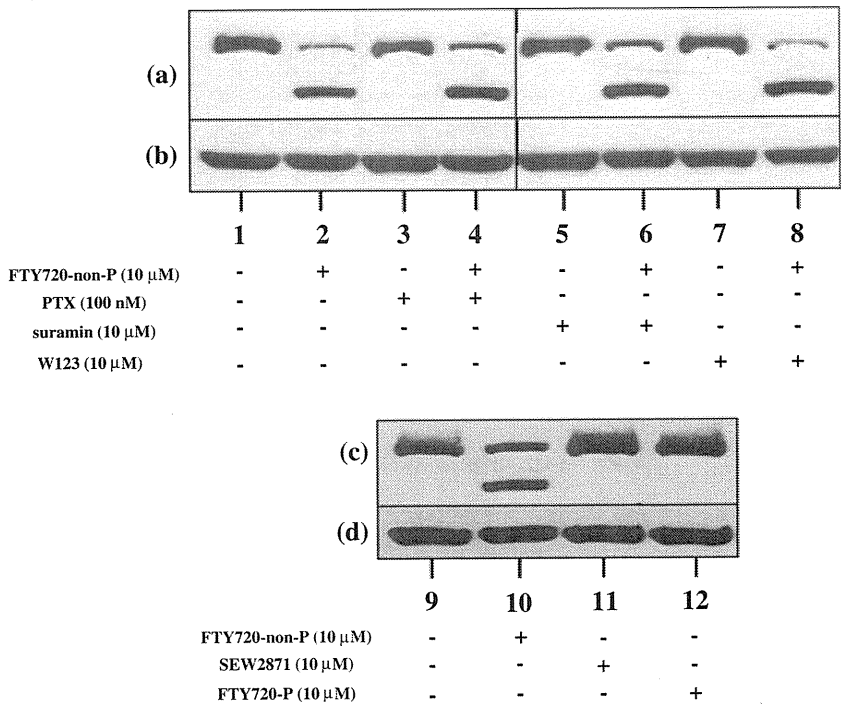

Fig. 4 FTY720-induced apoptosis of HMO6 was independent of S1P receptor binding. HMO6 cells were exposed for 12 h to 10 μM FTY720-non-P with or without inclusion of various S1P receptor agonists and antagonists. Pretreatment started at 30 min before exposure to FTY720-non-P. **a–d** indicate western blot of **a**, **c** PARP and **b**, **d** HSP60, an internal control of protein loading. The lanes (*1–12*) indicate (*1*, *9*) untreated HMO6 cells, and HMO6 cells treated with (*2*, *10*) 10 μM FTY720-non-P exposure alone, (*3*) 100 nM pertussis toxin (PTX) pretreatment alone, (4) 100 nM PTX pretreatment and 10 μM FTY720-non-P exposure, (*5*) 10 μM suramin pretreatment alone, (*6*) 10 μM suramin pretreatment and 10 μM FTY720-non-P exposure, (*7*) 10 μM W123 pretreatment alone, (*8*) 10 μM W123 pretreatment and 10 μM FTY720-non-P exposure, and HOM6 cells treated with a 12 h-exposure to (*11*) 10 μM SEW2871 or (*12*) 10 μM phosphorylated FTY720 (FTY720-P)

in HMO6 cells. The N-terminal fragment of SREBP2 is cleaved, dimerized, and translocated to the nucleus in response to the activating stimuli (Sato 2010). We identified the cleaved form of SREBP2 in HMO6 cells following an 1 h-exposure to FTY720-non-P ranging from 10 to 20 μM or by treatment with 3 μM simvastatin, a HMG-CoA reductase inhibitor capable of activating SREBP2 (Fig. 6a, lanes 2–4). Neither FTY720-non-P nor simvastatin alone at a concentration of 5 μM each induced apoptosis of HMO6 (Fig. 2a; Fig. 6b, lanes 7, 8). In contrast, a 12 h-pretreatment with 5 μM simvastatin enhanced FTY720-non-P-induced apoptosis of HMO6 cells, suggesting a proapoptotic effect mediated by SREBP2 activation following simvastatin treatment (Fig. 6b, lane 10).

A recent study showed that statins activate SREBP2, which positively controls the expression of caspase-7, resulting in induction of apoptosis of human gastric cancer cells (Gibot et al. 2009). When the N-terminal fragment of SREBP2 was overexpressed in HMO6 cells, the cleavage of PARP and caspase-3 was greatly enhanced, compared with the cells with overexpression of LacZ (Fig. 6c, f, lane 12), while the levels of procaspase-7 and cleaved caspase-7 were unaltered (Fig. 6g, lane 12).

Discussion

The present study revealed that non-phosphorylated FTY720 (FTY720-non-P) induced apoptosis of human microglia HM06 in a time- and dose-dependent manner with IC50 of 10.6 ± 2.0 μM. The apoptosis was inhibited by Z-DQMD-FMK, a caspase-3 inhibitor, but not by Pertussis toxin, a Gi protein inhibitor, suramin, a S1P3/S1P5 inhibitor, or W123, a S1P1 competitive antagonist, although HMO6 expressed S1P1, S1P2, and S1P3. Furthermore, both phosphorylated FTY720 (FTY720-P) and SEW2871, S1P1 selective agonists, did not induce apoptosis of HMO6. These observations suggest that FTY720-non-P-induced apoptosis of HMO6 cells is independent of S1P receptor binding.

Supporting these observations, FTY720, serving as a potential anti-cancer agent, induces apoptosis of various human cancer cell lines derived from liver, kidney, pancreas, and breast, multiple myeloma and leukemia cells, which is often mediated by S1P receptor-independent mechanisms (Matsuoka et al. 2003; Lee et al. 2004; Liu et al. 2010; Nagaoka et al. 2008). The concentrations required to induce apoptosis of tumor cells in vitro are about

Table 1 Upregulated genes in HMO6 following treatment with FTY720-non-P

Rank	Fold change	Entrez gene ID	Gene symbol	Gene name
1	5.75	25774	GSTTP1	Glutathione S-transferase theta pseudogene 1
2	3.16	150527	LOC150527	Hypothetical LOC150527
3	2.78	728380	RPL7P26	Ribosomal protein L7 pseudogene 26
4	2.74	3638	INSIG1	Insulin induced gene 1
5	2.72	158160	HSD17B7P2	Hydroxysteroid (17-beta) dehydrogenase 7 pseudogene 2
6	2.70	3157	HMGCS1	3-hydroxy-3-methylglutaryl-coenzyme A synthase 1 (soluble)
7	2.68	346007	EYS	Eyes shut homolog (Drosophila)
8	2.48	26834	RNU4-2	RNA, U4 small nuclear 2
9	2.46	163720	CYP4Z2P	Cytochrome P450, family 4, subfamily Z, polypeptide 2 pseudogene
10	2.44	54541	DDIT4	DNA-damage-inducible transcript 4
11	2.41	6351	CCL4	Chemokine (C–C motif) ligand 4
12	2.39	3949	LDLR	Low density lipoprotein receptor
13	2.37	6307	SC4MOL	Sterol-C4-methyl oxidase-like
14	2.34	286359	LOC286359	Hypothetical LOC286359
15	2.30	391003	PRAMEF18	PRAME family member 18
16	2.29	23175	LPIN1	Lipin 1
17	2.25	54897	CASZ1	Castor zinc finger 1
18	2.16	3156	HMGCR	3-hydroxy-3-methylglutaryl-coenzyme A reductase
19	2.16	196335	OR56B4	Olfactory receptor, family 56, subfamily B, member 4
20	2.10	3283	HSD3B1	Hydroxy-delta-5-steroid dehydrogenase, 3 beta- and steroid delta-isomerase 1
21	2.09	8553	BHLHE40	Basic helix-loop-helix family, member e40
22	2.07	10517	FBXW10	F-box and WD repeat domain containing 10
23	2.06	256892	OR51F1	Olfactory receptor, family 51, subfamily F, member 1
24	2.05	4598	MVK	Mevalonate kinase
25	2.04	196074	METT5D1	Methyltransferase 5 domain containing 1
26	2.04	901	CCNG2	Cyclin G2
27	2.03	439927	C1orf180	Chromosome 1 open reading frame 180
28	2.01	10551	AGR2	Anterior gradient homolog 2 (Xenopus laevis)
29	2.01	91074	ANKRD30A	Ankyrin repeat domain 30A
30	2.00	1831	TSC22D3	TSC22 domain family, member 3

HMO6 cells were exposed to non-phosporylated FTY720 (10 μM) or vehicle (DMSO) for 2 h. The genome-wide transcriptome was studied on Human Gene 1.0 ST array. The genes with an over 2-fold increase in FTY720-non-P-treated HMO6 cells are listed. The genes associated with steroid and/or sterol metabolism annotated by the DAVID program are underlined

two orders of magnitude greater than the blood concentration in the clinical setting, i.e., 5.4 ng/ml in plasma (Brinkmann et al. 2001, 2010). FTY720 has a half-life of approximately 10 days in vivo, and is cleared predominantly by a metabolic pathway requiring cytochrome P450 4F2 (CYP4F2) (Jin et al. 2011). The enzymatic activity of CYP4F2 is inhibited by certain drugs like ketoconazole, and the gene encoding CYP4F2 has a variety of single nucleotide polymorphisms (SNPs) (www.ncbi.nlm.nih.gov/snp). Therefore, in poor metabolizers of FTY720 receiving a CYP4F2 inhibitor, if they exist, the blood concentration of FTY720 could increase up to the range of toxic levels.

FTY720-non-P goes through the plasma membrane without requirement of the receptor binding, and targets directly key intracellular enzymes involved in sphingolipid metabolism, such as sphingosine kinases, phospholipase A2, and S1P lyase (Bandhuvula et al. 2005). FTY720 also inhibits ceramide synthases, resulting in a decrease in cellular levels of ceramide, dihydroceramide, shingosine, and S1P, and an increase in dihydrosphingosine and dihydroshingosine-1-phosphate, all of which alter the endogenous balance between survival and apoptotic signals (Berdyshev et al. 2009). FTY720-non-P promotes phosphorylation of 14-3-3zeta on Ser58 that disrupts 14-3-3 dimer formation, resulting in releasing proapototic mediators (Woodcock et al. 2010). FTY720, phosphorylated by SPHK2 located inside the plasma membrane, is transported outside the cells via the S1P transporter named spinster

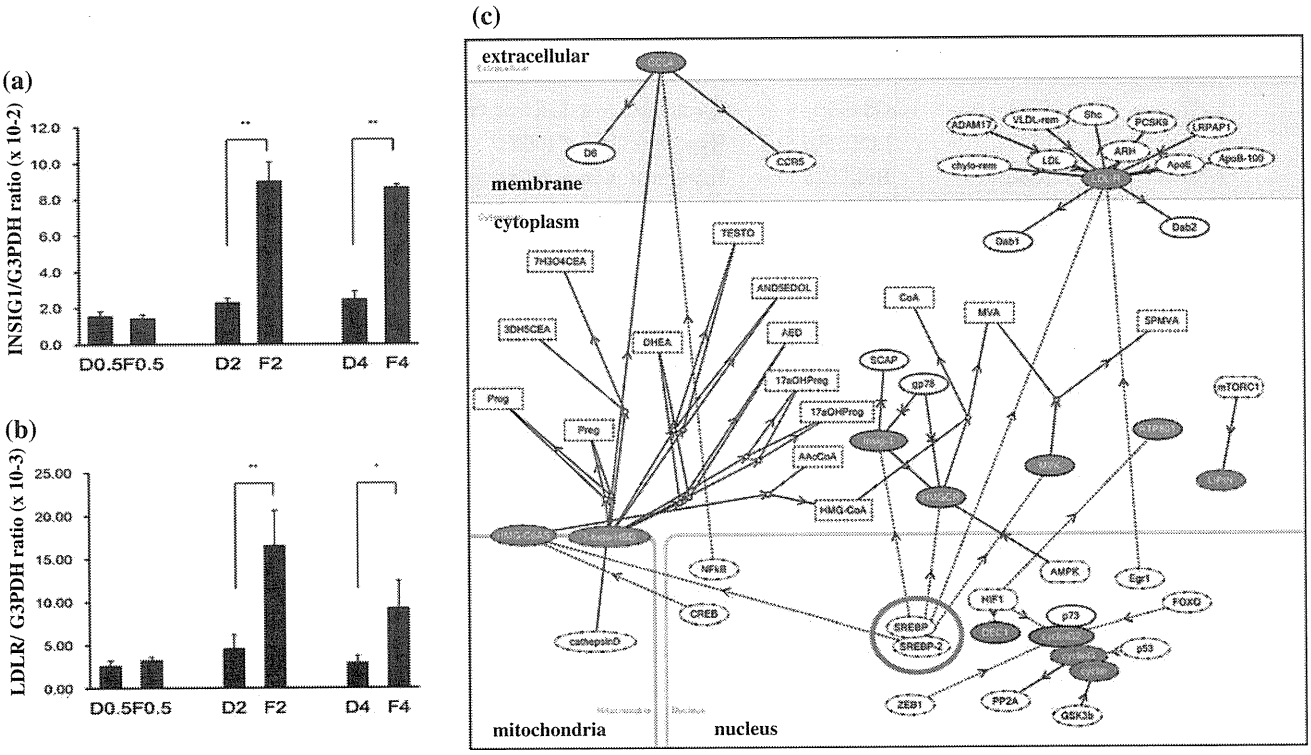

Fig. 5 FTY720 Induced SREBP-Responsive Genes. HMO6 cells were exposed for 2 h to 10 μM FTY720-non-P or vehicle (DMSO). Then, total RNA was processed for the genome-wide gene expression profiling on a microarray, followed by molecular network analysis by KeyMolnet and validation by qPCR. We identified 30 upregulated genes in FTY720-non-P-treated HMO6 cells (Table 1). **a–c** indicate qPCR of **a** INSIG1 and **b** LDLR, and **c** molecular network of FTY720-non-P-induced genes. Abbreviations: D, vehicle (DMSO); F, FTY720-non-P; 0.5, 30 min; 2, 2 h; and 4, 4 h. In **c**, red filled nodes represent FTY720-non-P-induced genes, whereas white open nodes exhibit additional nodes extracted automatically from the core contents of KeyMolnet to establish molecular connections. The molecular relation is indicated by solid line with arrow (direct binding or activation), solid line with arrow and stop (direct inactivation), solid line without arrow (complex formation), dash line with arrow (transcriptional activation), and dash line with arrow and stop (transcriptional repression). The transcription factor SREBP (SREBP2) is highlighted by a red thick circle

homolog 2 (SPNS2), and then the phosphorylated FTY720 binds to S1P receptors expressed on the surface of the plasma membrane (Hisano et al. 2011).

Being consistent with our observations, FTY720-non-P but not FTY720-P induces apoptosis of human breast and colon cancers (Nagaoka et al. 2008). FTY720 inhibits cytosolic phospholipase A2 ($cPLA_2$) in a manner independent of S1P receptor binding (Payne et al. 2007). FTY720-non-P but not FTY720-P inhibits PKC activation, which is associated with cell-surface expression of S1P1 (Sensken and Gräler 2010). Furthermore, FTY720-P counteracts FTY720-non-P-induced apoptosis of human fibroblasts by activating Bcl-2 (Potteck et al. 2010).

Several previous studies showed that FTY720-induced apoptosis is often accompanied by activation of a series of caspases (Wang et al. 1999). We found activation of both caspase-3 and caspase-7 during FTY720-non-P-induced apoptosis of HMO6. Furthermore, FTY720-induced apoptosis also involves various mechanisms, such as dephosphorylation of protein kinase B (Akt) (Matsuoka et al. 2003; Lee et al. 2004), deregulation of mitogen-activated protein kinases (MAPKs), focal adhesion kinase (FAK), and Rho-GTPase (Matsuda et al. 1999; Sonoda et al. 2001), and activation of protein phosphatase 2A (PP2A) (Liu et al. 2010). Here, we for the first time showed that FTY720-non-P-induced apoptosis of HMO6 cells is positively regulated by the SREBP2-dependent signaling pathway.

A recent study showed that statins induce apoptosis of human gastric cancer cells by activating SREBP1 and SREBP2, both of which transcriptionally upregulate caspase-7 (Gibot et al. 2009). Statin-dependent apoptosis is prevented by replenishment of mevalonate, the immediate product by the HMG-CoA reductase activity (Xia et al. 2001). A previous study showed that activation of caspase-3 releases SREBP proteins from ER membrane in a proteolytic reaction distinct from the sterol-regulated cleavage, resulting in nuclear transport of SREBP and transcriptional activation of sterol-regulatory genes (Higgins and Ioannou 2001). However, during FTY720-non-P-induced apoptosis of HMO6 cells, we identified activation of SREBP2 as early as at 1 h after initiation of the treatment, which is long before detection of the PARP cleavage, suggesting that

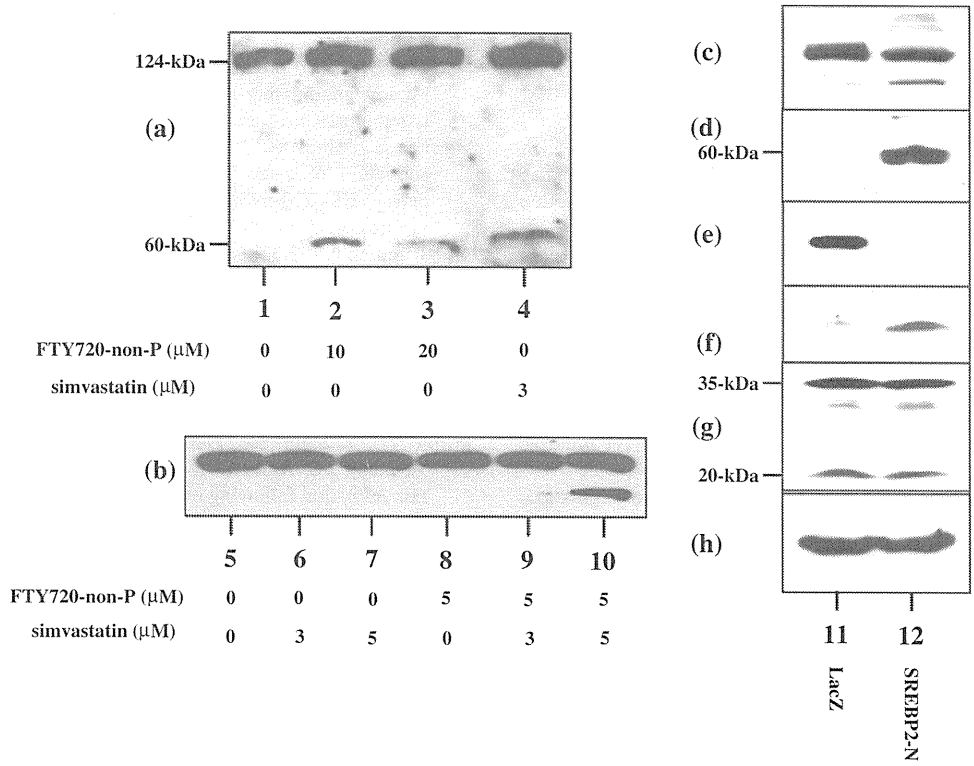

Fig. 6 Activation of SREBP2 by FTY720-non-P in HMO6 cells. HMO6 cells were exposed to FTY720-non-P or simvastatin, or transfected with the vector expressing the N-terminal fragment of SREBP2 (SREBP2-N) or LacZ. **a–h** indicate western blot of **a**, **d** SREBP2, **b**, **c** PARP, **e** V5, **f** cleaved caspase-3, **g** caspase-7 (a 35-kDa proform and a 20-kDa cleaved form), and **h** HSP60. The lanes *1–12* represent (*1*, *5*) untreated HMO6 cells, and HMO6 cells treated for 1 h with (*2*) 10 μM FTY720-non-P, (*3*) 20 μM FTY720-non-P, (*4*) 3 μM simvastatin, and HMO6 cells pretreated for simvastatin starting at 12 h before a 6 h-exposure to FTY720-non-P, whose conditions are composed of (*6*) 3 μM simvastatin pretreatment alone, (*7*) 5 μM simvastatin pretreatment alone, (*8*) no simvastatin pretreatment and 5 μM FTY720-non-P exposure, (*9*) 3 μM simvastatin pretreatment and 5 μM FTY720-non-P exposure, and (*10*) 5 μM simvastatin pretreatment and 5 μM FTY720-non-P exposure, and HMO6 cells with overexpression of (*11*) V5-tagged LacZ or (*12*) SREBP2-N

SREBP activation is not a secondary phenomenon following caspase-3 activation. Furthermore, we found that activation of SREBP2 by overexpression of the N-terminal fragment of SREBP2 in HMO6 cells enhances the cleavage of PARP and caspase-3 in the absence of FTY720. Moreover, we found that pretreatment with simvastatin enhanced FTY720-non-P-induced apoptosis of HMO6 cells. Statins activate SREBP2 and induce apoptosis of various cells (Xia et al. 2001; Gibot et al. 2009). All of these observations suggest that the SREBP2-dependent signaling pathway is intrinsically proapoptotic, when it is aberrantly regulated.

A recent study showed that FTY720 inhibits intracellular transport of cholesterol to ER in human macrophages, being independent of S1P1 binding, indicating that FTY720-non-P certainly affects the cellular cholesterol processing (Blom et al. 2010). Importantly, cholesterol interacts specifically with sphingosine in human intestinal epithelial cells under physiological conditions (Garmy et al. 2005). S1P is intracellularly generated by sphingosine kinases SPHK1 and SPHK2 from sphingosine, a breakdown product of the cell membrane constituent sphingomyelin (Chi 2011). S1P and its synthetic analog FTY720-P share S1P1, S1P3, S1P4, and S1P5 expressed on the plasma membrane. All of these observations propose a possible scenario that excessive amounts of intracellular FTY720-non-P disturb the complex metabolic network of cholesterols and sphingolipids, resulting in activation of the SREBP2-dependent proapoptotic signaling pathway.

Acknowledgments This work was supported by grants from the Research on Intractable Diseases, the Ministry of Health, Labour and Welfare, Japan (H22-Nanchi-Ippan-136; H21-Nanchi-Ippan-201; H21-Nanchi Ippan-217; H21-Kokoro-Ippan-018) and the High-Tech Research Center Project (S0801043) and the Grant-in-Aid (C22500322), the Ministry of Education, Culture, Sports, Science and Technology (MEXT), Japan. The microarray data are available from Gene Expression Omnibus (GEO) under the accession number GSE28642.

References

Bandhuvula P, Tam YY, Oskouian B, Saba JD (2005) The immune modulator FTY720 inhibits sphingosine-1-phosphate lyase activity. J Biol Chem 280:33697–33700

Berdyshev EV, Gorshkova I, Skobeleva A, Bittman R, Lu X, Dudek SM, Mirzapoiazova T, Garcia JG, Natarajan V (2009) FTY720 inhibits ceramide synthases and up-regulates dihydrosphingosine 1-phosphate formation in human lung endothelial cells. J Biol Chem 284:5467–5477

Blom T, Bäck N, Mutka AL, Bittman R, Li Z, de Lera A, Kovanen PT, Diczfalusy U, Ikonen E (2010) FTY720 stimulates 27-hydroxycholesterol production and confers atheroprotective effects in human primary macrophages. Circ Res 106:720–729

Brinkmann V, Wilt C, Kristofic C, Nikolova Z, Hof RP, Chen S, Albert R, Cottens S (2001) FTY720: dissection of membrane receptor-operated, stereospecific effects on cell migration from receptor-independent antiproliferative and apoptotic effects. Transplant Proc 33:3078–3080

Brinkmann V, Billich A, Baumruker T, Heining P, Schmouder R, Francis G, Aradhye S, Burtin P (2010) Fingolimod (FTY720): discovery and development of an oral drug to treat multiple sclerosis. Nat Rev Drug Discov 9:883–897

Chi H (2011) Sphingosine-1-phosphate and immune regulation: trafficking and beyond. Trends Pharmacol Sci 32:16–24

Choi JW, Gardell SE, Herr DR, Rivera R, Lee CW, Noguchi K, Teo ST, Yung YC, Lu M, Kennedy G, Chun J (2011) FTY720 (fingolimod) efficacy in an animal model of multiple sclerosis requires astrocyte sphingosine 1-phosphate receptor 1 (S1P1) modulation. Proc Natl Acad Sci USA 108:751–756

Coelho RP, Payne SG, Bittman R, Spiegel S, Sato-Bigbee C (2007) The immunomodulator FTY720 has a direct cytoprotective effect in oligodendrocyte progenitors. J Pharmacol Exp Ther 323:626–635

da Huang W, Sherman BT, Lempicki RA (2009) Systematic and integrative analysis of large gene lists using DAVID bioinformatics resources. Nat Protoc 4:44–57

Dev KK, Mullershausen F, Mattes H, Kuhn RR, Bilbe G, Hoyer D, Mir A (2008) Brain sphingosine-1-phosphate receptors: implication for FTY720 in the treatment of multiple sclerosis. Pharmacol Ther 117:77–93

Durafourt BA, Lambert C, Johnson TA, Blain M, Bar-Or A, Antel JP (2011) Differential responses of human microglia and blood-derived myeloid cells to FTY720. J Neuroimmunol 230:10–16

Garmy N, Taïeb N, Yahi N, Fantini J (2005) Interaction of cholesterol with sphingosine: physicochemical characterization and impact on intestinal absorption. J Lipid Res 46:36–45

Gibot L, Follet J, Metges JP, Auvray P, Simon B, Corcos L, Le Jossic-Corcos C (2009) Human caspase 7 is positively controlled by SREBP-1 and SREBP-2. Biochem J 420:473–483

Higgins ME, Ioannou YA (2001) Apoptosis-induced release of mature sterol regulatory element-binding proteins activates sterol-responsive genes. J Lipid Res 42:1939–1946

Hisano Y, Kobayashi N, Kawahara A, Yamaguchi A, Nishi T (2011) The sphingosine 1-phosphate transporter, SPNS2, functions as a transporter of the phosphorylated form of the immunomodulating agent FTY720. J Biol Chem 286:1758–1766

Jack C, Ruffini F, Bar-Or A, Antel JP (2005) Microglia and multiple sclerosis. J Neurosci Res 81:363–373

Jin Y, Zollinger M, Borell H, Zimmerlin A, Patten CJ (2011) CYP4F enzymes are responsible for the elimination of fingolimod (FTY720), a novel treatment of relapsing multiple sclerosis. Drug Metab Dispos 39:191–198

Kappos L, Antel J, Comi G, Montalban X, O'Connor P, Polman CH, Haas T, Korn AA, Karlsson G, Radue EW, FTY720 D2201 Study Group (2006) Oral fingolimod (FTY720) for relapsing multiple sclerosis. N Engl J Med 355:1124–1140

Lee TK, Man K, Ho JW, Sun CK, Ng KT, Wang XH, Wong YC, Ng IO, Xu R, Fan ST (2004) FTY720 induces apoptosis of human hepatoma cell lines through PI3-K-mediated Akt dephosphorylation. Carcinogenesis 25:2397–2405

Liu Q, Alinari L, Chen CS, Yan F, Dalton JT, Lapalombella R, Zhang X, Mani R, Lin T, Byrd JC, Baiocchi RA, Muthusamy N (2010) FTY720 shows promising in vitro and in vivo preclinical activity by downmodulating cyclin D1 and phospho-Akt in mantle cell lymphoma. Clin Cancer Res 16:3182–3192

Matsuda S, Minowa A, Suzuki S, Koyasu S (1999) Differential activation of c-Jun NH2-terminal kinase and p38 pathways during FTY720-induced apoptosis of T lymphocytes that is suppressed by the extracellular signal-regulated kinase pathway. J Immunol 162:3321–3326

Matsuoka Y, Nagahara Y, Ikekita M, Shinomiya T (2003) A novel immunosuppressive agent FTY720 induced Akt dephosphorylation in leukemia cells. Br J Pharmacol 138:1303–1312

Miron VE, Jung CG, Kim HJ, Kennedy TE, Soliven B, Antel JP (2008) FTY720 modulates human oligodendrocyte progenitor process extension and survival. Ann Neurol 63:61–71

Miron VE, Ludwin SK, Darlington PJ, Jarjour AA, Soliven B, Kennedy TE, Antel JP (2010) Fingolimod (FTY720) enhances remyelination following demyelination of organotypic cerebellar slices. Am J Pathol 176:2682–2694

Mullershausen F, Zecri F, Cetin C, Billich A, Guerini D, Seuwen K (2009) Persistent signaling induced by FTY720-phosphate is mediated by internalized S1P1 receptors. Nat Chem Biol 5: 428–434

Nagai A, Nakagawa E, Hatori K, Choi HB, McLarnon JG, Lee MA, Kim SU (2001) Generation and characterization of immortalized human microglial cell lines: expression of cytokines and chemokines. Neurobiol Dis 8:1057–1068

Nagaoka Y, Otsuki K, Fujita T, Uesato S (2008) Effects of phosphorylation of immunomodulatory agent FTY720 (fingolimod) on antiproliferative activity against breast and colon cancer cells. Biol Pharm Bull 31:1177–1181

Narantuya D, Nagai A, Sheikh AM, Masuda J, Kobayashi S, Yamaguchi S, Kim SU (2010) Human microglia transplanted in rat focal ischemia brain induce neuroprotection and behavioral improvement. PLoS One 5:e11746

Payne SG, Oskeritzian CA, Griffiths R, Subramanian P, Barbour SE, Chalfant CE, Milstien S, Spiegel S (2007) The immunosuppressant drug FTY720 inhibits cytosolic phospholipase A2 independently of sphingosine-1-phosphate receptors. Blood 109: 1077–1085

Potteck H, Nieuwenhuis B, Lüth A, van der Giet M, Kleuser B (2010) Phosphorylation of the immunomodulator FTY720 inhibits programmed cell death of fibroblasts via the S1P3 receptor subtype and Bcl-2 activation. Cell Physiol Biochem 26:67–78

Sato R (2010) Sterol metabolism and SREBP activation. Arch Biochem Biophys 501:177–181

Satoh J, Tabunoki H, Arima K (2009) Molecular network analysis suggests aberrant CREB-mediated gene regulation in the Alzheimer disease hippocampus. Dis Markers 27:239–252

Sensken SC, Gräler MH (2010) Down-regulation of S1P1 receptor surface expression by protein kinase C inhibition. J Biol Chem 285:6298–6307

Sonoda Y, Yamamoto D, Sakurai S, Hasegawa M, Aizu-Yokota E, Momoi T, Kasahara T (2001) FTY720, a novel immunosuppressive agent, induces apoptosis in human glioma cells. Biochem Biophys Res Commun 281:282–288

Van Doorn R, Van Horssen J, Verzijl D, Witte M, Ronken E, Van Het Hof B, Lakeman K, Dijkstra CD, Van Der Valk P, Reijerkerk A, Alewijnse AE, Peters SL, De Vries HE (2010) Sphingosine 1-phosphate receptor 1 and 3 are upregulated in multiple sclerosis lesions. Glia 58:1465–1476

Wang JD, Takahara S, Nonomura N, Ichimaru N, Toki K, Azuma H, Matsumiya K, Okuyama A, Suzuki S (1999) Early induction of apoptosis in androgen-independent prostate cancer cell line by FTY720 requires caspase-3 activation. Prostate 40:50–55

Wei Y, Yemisci M, Kim HH, Yung LM, Shin HK, Hwang SK, Guo S, Qin T, Alsharif N, Brinkmann V, Liao JK, Lo EH, Waeber C (2011) Fingolimod provides long-term protection in rodent models of cerebral ischemia. Ann Neurol 69:119–129

Woodcock JM, Ma Y, Coolen C, Pham D, Jones C, Lopez AF, Pitson SM (2010) Sphingosine and FTY720 directly bind pro-survival 14-3-3 proteins to regulate their function. Cell Signal 22: 1291–1299

Xia Z, Tan MM, Wong WW, Dimitroulakos J, Minden MD, Penn LZ (2001) Blocking protein geranylgeranylation is essential for lovastatin-induced apoptosis of human acute myeloid leukemia cells. Leukemia 15:1398–1407

Zhang Z, Zhang Z, Fauser U, Artelt M, Burnet M, Schluesener HJ (2007) FTY720 attenuates accumulation of EMAP-II+ and MHC-II+ monocytes in early lesions of rat traumatic brain injury. J Cell Mol Med 11:307–314

BioData Mining

RESEARCH Open Access

Comprehensive analysis of human microRNA target networks

Jun-ichi Satoh* and Hiroko Tabunoki

* Correspondence: satoj@my-pharm.ac.jp
Department of Bioinformatics and Molecular Neuropathology, Meiji Pharmaceutical University, 2-522-1 Noshio, Kiyose, Tokyo 204-8588, Japan

Abstract

Background: MicroRNAs (miRNAs) mediate posttranscriptional regulation of protein-coding genes by binding to the 3' untranslated region of target mRNAs, leading to translational inhibition, mRNA destabilization or degradation, depending on the degree of sequence complementarity. In general, a single miRNA concurrently downregulates hundreds of target mRNAs. Thus, miRNAs play a key role in fine-tuning of diverse cellular functions, such as development, differentiation, proliferation, apoptosis and metabolism. However, it remains to be fully elucidated whether a set of miRNA target genes regulated by an individual miRNA in the whole human microRNAome generally constitute the biological network of functionally-associated molecules or simply reflect a random set of functionally-independent genes.

Methods: The complete set of human miRNAs was downloaded from miRBase Release 16. We explored target genes of individual miRNA by using the Diana-microT 3.0 target prediction program, and selected the genes with the miTG score ≧ 20 as the set of highly reliable targets. Then, Entrez Gene IDs of miRNA target genes were uploaded onto KeyMolnet, a tool for analyzing molecular interactions on the comprehensive knowledgebase by the neighboring network-search algorithm. The generated network, compared side by side with human canonical networks of the KeyMolnet library, composed of 430 pathways, 885 diseases, and 208 pathological events, enabled us to identify the canonical network with the most significant relevance to the extracted network.

Results: Among 1,223 human miRNAs examined, Diana-microT 3.0 predicted reliable targets from 273 miRNAs. Among them, KeyMolnet successfully extracted molecular networks from 232 miRNAs. The most relevant pathway is transcriptional regulation by transcription factors RB/E2F, the disease is adult T cell lymphoma/leukemia, and the pathological event is cancer.

Conclusion: The predicted targets derived from approximately 20% of all human miRNAs constructed biologically meaningful molecular networks, supporting the view that a set of miRNA targets regulated by a single miRNA generally constitute the biological network of functionally-associated molecules in human cells.